Smith, C., Petsch, J., Schmidt, P. G., & Agris, P. F. (1985) *Biochemistry 24*, 1434–1440.
Sussman, J. L., Holbrook, S. R., Warrant, R. W., Church, G. M., & Kim, S. H. (1978) *J. Mol. Biol. 123*, 601–630.
Tompson, J. G., & Agris, P. F. (1979) *Nucleic Acids Res. 7*, 765–779.
Tompson, J. G., Hayashi, F., Paukstelis, J. V., Loeppky, R. N., & Agris, P. F. (1979) *Biochemistry 18*, 2029–2085.

NMR Studies of Conformations and Interactions of Substrates and Ribonucleotide Templates Bound to the Large Fragment of DNA Polymerase I†

Lance J. Ferrin and Albert S. Mildvan*
Department of Biological Chemistry, Johns Hopkins University School of Medicine, Baltimore, Maryland 21205
Received December 26, 1985; Revised Manuscript Received March 20, 1986

ABSTRACT: The large fragment of DNA polymerase I (Pol I) effectively uses oligoribouridylates and oligoriboadenylates as templates, with kinetic properties similar to those of poly(U) and poly(A), respectively, and has little or no activity in degrading them. In the presence of such oligoribonucleotide templates, nuclear Overhauser effects (NOE's) were used to determine interproton distances within and conformations of substrates bound to the large fragment of Pol I, as well as conformations and interactions of the enzyme-bound templates. In the enzyme–oligo$(rU)_{54\pm11}$–Mg^{2+}dATP complex, the substrate dATP has a high anti-glycosidic torsional angle ($\chi = 62 \pm 10°$) and an O1′-endo/C3′-endo sugar pucker ($\delta = 90 \pm 10°$) differing only slightly from those previously found for enzyme-bound dATP in the absence of template [Ferrin, L. J., & Mildvan, A. S. (1985) *Biochemistry 24*, 4680–4694]. Both conformations are similar to those of deoxynucleotidyl units of B DNA but differ greatly from those of A or Z DNA. The conformation of the enzyme-bound substrate analogue AMPCPP ($\chi = 50 \pm 10°$, $\delta = 90 \pm 10°$) is very similar to that of enzyme-bound dATP and is unaltered by the binding of the template oligo$(rU)_{54\pm11}$ or by the subsequent binding of the primer $(Ap)_9A$. In the enzyme–oligo$(rA)_{50}$–Mg^{2+}TTP complex, the substrate TTP has an anti-glycosidic torsional angle ($\chi = 40 \pm 10°$) and an O1′-endo sugar pucker ($\delta = 100 \pm 10°$), indistinguishable from those found in the absence of template and compatible with those of B DNA but not with those of A or Z DNA. In the absence of templates, the interproton distances on enzyme-bound dGTP cannot be fit by a single conformation but require a 40% contribution from a syn structure ($\chi = 222°$) and a 60% contribution from one or more anti structures. The presence of the template oligo$(rU)_{43\pm9}$ simplifies the conformation of enzyme-bound dGTP to a single structure with an *anti*-glycosyl angle ($\chi = 32 \pm 10°$) and an O1′-endo/C3′-endo sugar pucker ($\delta = 90 \pm 10°$), compatible with those of B DNA, possibly due to the formation of a G-U wobble base pair. However, no significant misincorporation of guanine deoxynucleotides by the enzyme is detected with oligo(rU) as template. Mutual substrate displacement experiments show that the presence of templates and primer does not alter the relative affinities of the enzyme for complementary and noncomplementary substrates. Hence, a step subsequent to substrate binding and prior to DNA chain elongation is required to explain the high fidelity of template replication by Pol I. NOE studies reveal the average nucleotidyl unit of free oligo$(rU)_{54\pm11}$ to be of a high anti angle ($\chi = 70 \pm 10°$) with an O1′ ribose pucker ($\delta = 105 \pm 10°$). The binding of oligo$(rU)_{54\pm11}$ to the enzyme broadens the resonances of the oligonucleotide and slightly alters the average glycosyl angle ($\chi = 60 \pm 10°$), but the conformation remains B-like. The binding of oligo$(rA)_{50\pm13}$ to the enzyme broadens the resonances of the oligonucleotide and causes small downfield shifts of the adenine resonances consistent with decreases in base stacking as occur in the transition from the A to the B conformation. NOE studies reveal the average adenyl unit of enzyme-bound oligo$(rA)_{50\pm13}$ to be anti, ruling out the Z conformation. Intermolecular NOE's from proton resonances of the enzyme to those of the substrate analogue AMPCPP reveal the proximity of hydrophobic amino acids with chemical shifts over the range 0.6–1.8 ppm and an aromatic amino acid at 6.80 ppm, most likely a Tyr residue. Intermolecular NOE's from proton resonances of the enzyme at 0.80, 1.55, 1.92, and 3.05 ppm to those of the bound oligo(rU) and oligo(rA) templates are most simply explained by the proximity of cationic Arg and/or Lys residues and possibly a hydrophobic residue.

DNA polymerase (Pol I)[1] from *Escherichia coli* and its large fragment have been the subject of extensive study by the techniques of classical enzymology (Kornberg, 1980, 1982), X-ray crystallography (Ollis et al., 1985), NMR (Slater et al., 1972; Sloan et al., 1975; Ferrin & Mildvan 1985a,b), transient-state kinetics (Bryant et al., 1983; Mizrahi et al., 1985), and chemical and genetic modification (Joyce et al., 1985a,b) in order to learn the mechanism by which this enzyme catalyzes the accurate copying of DNA. The cloning of the large fragment of Pol I in a high-expression vector

†This work was supported by National Institutes of Health Grant AM28616 and National Science Foundation Grant PCM8219464. L.J.F. is an awardee of the Medical Scientist Training Program (5T32GM07309).

[1] Abbreviations: Pol I, *Escherichia coli* DNA polymerase I; NOE, nuclear Overhauser effect; PEI, poly(ethylenimine); pH*, meter reading in ^2H_2O; A/D, analogue to digital conversion; DSS, sodium 4,4-dimethyl-4-silapentanesulfonate; AMPCPP, adenosine 5′-(α,β-methylene-triphosphate); SDS, sodium dodecyl sulfate; EDTA, ethylenediaminetetraacetic acid; Tris-HCl, tris(hydroxymethyl)aminomethane hydrochloride.

0006-2960/86/0425-5131$01.50/0

(Joyce & Grindley, 1983) has greatly facilitated such mechanistic studies.

Both Pol I (Englund et al., 1969a) and its large fragment (Ferrin & Mildvan, 1985b), in the presence of the divalent cation activator, are known to bind deoxynucleoside triphosphate substrates competitively at a single site. In previous papers, we have used NMR methods to determine the conformations and environments of the substrates dATP and TTP bound to Pol I and its large fragment (Sloan et al., 1985; Ferrin & Mildvan, 1985b). Metal to proton distances and interproton distances were consistent with unique conformations of the bound substrates that were appropriate for nucleotidyl units of B DNA. Intermolecular NOE's established the presence of at least two hydrophobic amino acids, probably including Ile, and an aromatic amino acid at the substrate binding site (Ferrin & Mildvan, 1985b). All of these studies were carried out in the absence of template and primer. This paper extends our studies of substrate conformations on the large fragment of Pol I by including templates and a primer. Moreover, information is also obtained on the conformations and environments of the bound templates. For these studies, in order to avoid hydrolysis, oligoribonucleotide templates and primers were used together with the large fragment of Pol I. A preliminary report of this work has been published (Ferrin & Mildvan, 1985a).

Experimental Procedures

Materials

Terminal deoxynucleotidyl transferase and oligo(dT)$_{50}$ were the gifts of F. Bollum. 2′-Deoxyadenosine 5′-*O*-(1-thiotriphosphate) (αSdATP) and 2′-deoxythymidine 5′-*O*-(1-thiotriphosphate) (αSTTP) were the gifts of F. Eckstein. [^{3}H]-dGTP was the gift of L. Loeb. ^{32}P-Labeled fragments of a *Hpa*II digest of the plasmid pBR322 were the gift of B. Sollner-Webb. *Escherichia coli* strain (CJ155), which overproduces the large fragment of DNA polymerase I, was generously provided by N. Grindley.

Yeast tRNA^{Phe} and adenosine 5′-(α,β-methylenetriphosphate) (AMPCPP) were purchased from Sigma. All deoxynucleoside triphosphates, the oligonucleotide primers (Ap)$_9$A, (dA)$_{10}$, (dA)$_{12-18}$, and (dT)$_{10}$, the polynucleotides poly(rU), poly(rA), and poly(dAT), and S_1 nuclease were purchased from P-L Biochemicals. PEI–cellulose plates were purchased from J. T. Baker or Sigma. Chelex-100 was purchased from Bio-Rad and was converted to the K^+ form before use. Ultrapure $MgCl_2$ was purchased from Accurate Chemical and Scientific Corp.; 99.96% ^2H_2O was purchased from Wilmad, and 99.8% ^2H_2O was purchased from Stohler and was sublimed under vacuum to remove a small amount of a white amorphous impurity.

Methods

Purification of the Large Fragment of Pol I. The large fragment of DNA polymerase I was purified to homogeneity from *E. coli* strain CJ155 by the method of Joyce and Grindley (1983), including their optional gel filtration step on Sephacryl S-200 to remove whole Pol I. This step was found to be necessary to remove trace amounts (<1%) of whole Pol I, as detected by SDS–polyacrylamide gel electrophoresis of early fractions on overloaded gels. These early fractions constituting 40% of the total protein, while unaltered in specific activity, were not used for NMR experiments. The specific activities of the two preparations of the large fragment used in these studies were both 15 000 units/mg as assayed by the method of Setlow (1974), and the conformations of enzyme-bound TTP on both preparations as determined by NMR (Ferrin & Mildvan, 1985b) were indistinguishable.

Testing of Blocked Oligonucleotides for Protection against the 3′–5′ Exonuclease of the Large Fragment. In order to study the conformation of deoxynucleoside triphosphates in the presence of the large fragment and templates, it was first necessary to find a template that was sufficiently stable to the 3′–5′ exonuclease of the large fragment. Such a template should be at least about 19 nucleotides in length, since the large fragment protects that many in DNase I footprinting experiments (Joyce et al., 1985b). The length, however, should not be so long as to cause large viscosity changes at the high concentrations required for NMR analysis. Hence, we chose a length of ~50 base pairs. Analogous reasoning led to the choice of 60 ± 5 base pairs for an NMR study of the RNA polymerase–poly(dAT) complex by Chatterji et al. (1984). The 3′ end of (dT)$_{50}$ was blocked with either dideoxythymidine 5′-triphosphate or αSTTP by use of terminal deoxynucleotidyl transferase and a modification of the procedure of Bollum (1974). The blocked polymer (10–14 μM) was then incubated with the large fragment of Pol I (8 μM) under buffer and Mg^{2+} concentrations to be used in the NMR experiments, and the nucleotides generated by the exonuclease activity were qualitatively monitored by thin-layer chromatography on PEI–cellulose plates run in 1.0 M LiCl, pH 7.0. The results showed these polymers to be unsuitable for NMR studies since it could be estimated that a stoichiometric complex of polymer and enzyme would result in complete degradation of the template in at most 1.5 h. Similar exonuclease studies with poly(rAU), poly(rU), and oligo(rU)$_{50}$ were quite promising, showing at least an order of magnitude greater stability of ribonucleotide polymers to hydrolysis.

Preparation of Oligoribonucleotide Templates. Oligoribonucleotides with a chain length of about 50 residues were prepared by alkaline degradation of poly(rA) and poly(rU) (Bock, 1967). The solutions contained 125 mg of homopolymer at a concentration of 1.0 mg/mL, 1.0 mM EDTA, and 100 mM NH_4HCO_3, pH 10.1. The solutions were then heated in a water bath until sufficient alkaline cleavage had occurred to reduce the average size of the polynucleotides to about 50 residues. About 4 h at 60 °C for poly(rU) or 50 min at 80 °C for poly(rA) was sufficient. The solutions were then cooled on ice and neutralized to pH 7.0 by the addition of 1.0 M HCl while being rapidly stirred. The oligonucleotides were precipitated by the addition of solid NaCl to a concentration of 0.1 M followed by 2.5 volumes of ethanol. After storage for at least 1 h in a −70 °C freezer to ensure complete precipitation, the oligonucleotides were collected by centrifugation at 4 °C.

Oligo(rU) was redissolved in a minimal volume of 10 mM Tris-HCl, pH 7.5, containing 1 mM EDTA and was fractionated on a 2.5 × 50 cm column of Sephadex G-100 (superfine) equilibrated at 4 °C with 75 mM NH_4OAc, pH 7.0. The column was run with the same buffer at a flow rate of 2 mL/h. A faster flow rate (10 mL/h) seriously compromised the resolution of the column. Oligo(rA) was redissolved and fractionated in 10 mM Tris-HCl, pH 7.5, and 100 mM NaCl otherwise as described for oligo(rU). A column run with the 75 mM NH_4OAc buffer led to very poor resolution of oligo(rA), possibly due to its aggregation in this buffer.

After fractionation, the oligonucleotides were examined on 6% polyacrylamide gels containing 7 M urea by the method of Maniatis et al. (1975). Yeast tRNA^{Phe}, its S_1 nuclease fragments (Rushizky & Mozejko, 1977), and a ^{32}P-labeled *Hpa*II digest of pBR322 were used as standards. Bands were visualized by UV irradiation of gels over fluorescent plates

(PEI–cellulose, Sigma or J. T. Baker) or by staining with 0.1% methylene blue. The relevant fractions were pooled and concentrated by ethanol precipitation in 0.1 M NaCl as before. Each pool generally contained ~10% of the total material. In the case of oligo(rU), the oligomer was run down a 1.3 × 20 cm column of Sephadex G-25, equilibrated at 4 °C with 10 mM Tris-HCl, pH 7.50, to remove all residual NH_4OAc. The Tris-HCl was removed by ethanol precipitation in 0.1 M NaCl. All oligomers were passed through Chelex-100 columns prior to storage to remove trace metal contaminants and were stored at −20 °C. Prior to use in an NMR experiment, the oligomers were lyophilized to dryness from H_2O and additionally lyophilized to dryness from ^2H_2O 1–3 times, although a single lyophilization was found to be sufficient to reduce the H_2O content to acceptable levels.

NMR Sample Conditions and Concentrations. All NMR experiments were carried out in deuterated 10 mM Tris-HCl, pH* 7.10, and 32 mM KCl at 24 °C. All NMR solutions, with the exception of those containing either Mg^{2+} or enzyme were passed through Chelex-100 prior to deuteration to remove trace metal impurities. The concentration of free Mg^{2+} necessary for optimal activity of whole Pol I was found by Travaglini et al. (1975) to range from 0.3 to 2.0 mM, depending on the template used. Repetition of their study with the large fragment of Pol I in 10 mM Tris-HCl, pH 7.50, and 32 mM KCl using oligo$(rU)_{54\pm11}$ as template and dA_{12-18} as the primer yielded a fairly broad Mg^{2+} optimum of 1.0–1.7 mM in excess of the deoxynucleoside triphosphate concentration. Consequently, all NMR experiments involving oligo(rU) as a template were done within this range. The exact concentrations of all components are given in the figure and table legends. The converse experiment with oligo$(rA)_{50\pm13}$ as template and $(dT)_{12}$ as primer yielded a Mg^{2+} optimum of 2.0 mM in excess of deoxynucleoside triphosphate concentration, with >90% activity between the range of 0.9–3.0 mM. This is in exact agreement with the results of Travaglini et al. (1975) with whole Pol I. Consequently, all NMR experiments involving oligo(rA) as a template were done at 2.0 mM Mg^{2+} in excess of deoxynucleoside triphosphate concentration. Oligonucleotide conformations and interactions were usually measured in the absence of Mg^{2+} to avoid degradation. Englund et al. (1969b) demonstrated that binding of oligonucleotides to DNA polymerase I is not Mg^{2+} dependent. The effects of Mg^{2+} on oligonucleotide conformation and interactions were tested with the large fragment–oligo$(rA)_{50\pm13}$ complex. In this system, the addition of 2.0 mM Mg^{2+} produced little or no change in the longitudinal, transverse, or cross-relaxation rates of the protons of oligo$(rA)_{50\pm13}$.

The concentrations of the oligonucleotides, approximately 50 residues in length, were determined spectrophotometrically with the molar extinction coefficients per residue of the homopolymers $\epsilon_{260} = 8.9 \times 10^3$ and 9.4×10^3 for poly(rU) and poly(rA), respectively. The concentration of the decamer $(Ap)_9A$ was calculated with $\epsilon_{257} = 11.0 \times 10^3$ (Leng & Felsenfeld, 1966; Singer et al., 1962). The concentration of AMPCPP was determined with $\epsilon_{259} = 14.4 \times 10^3$. The concentrations of all components used in each experiment are given in the legends to the figures and the tables.

Kinetic Studies. Kinetic assays were carried out under conditions designed to duplicate the NMR conditions. All assays were carried out in 10 mM Tris-HCl, pH 7.5, and 32 mM KCl, at 24 °C. The concentration of Mg^{2+} in excess of nucleotide was 1.0 mM when oligo(rU) was used as the template and 2.0 mM when oligo(rA) was used as the template. In some assays, where large dilutions of the enzyme were required, bovine serum albumin was included in the enzyme diluent so that the final concentration of protein in the assay was never below 50 μg/mL. Assays were performed with DE-81 paper (Whatman) by the method of Brutlag & Kornberg (1972) as modified by Bryant et al. (1983).

NMR Spectroscopy. The equipment and pulse sequences used were as previously reported (Ferrin & Mildvan, 1985b; Rosevear et al., 1983). As before, the NOE's were measured by the truncated driven NOE method (Wagner & Wuthrich, 1979), which is especially useful in distinguishing primary from higher order NOE's.

The proton decoupler was utilized to produce the selective preirradiation pulse of duration t, between 0.15 and 1.0 s for enzyme-bound deoxynucleoside triphosphates and 0.04–0.2 s for enzyme-bound oligonucleotides. The shorter preirradiation times for the oligonucleotides were necessary because secondary NOE effects started to appear much earlier. A preirradiation time between 0.13 and 1.0 s was useful for oligo$(rU)_{54\pm11}$ in the absence of enzyme. A pulse power of 10 μW was used in determining the conformation of the enzyme-bound deoxynucleoside triphosphates, AMPCPP, and oligo$(rU)_{54\pm11}$ in the absence of enzyme. A pulse power of 20 μW was used in determining the conformation of enzyme-bound oligonucleotides. A pulse power of 20 μW for 0.5 s was used in obtaining the "action spectra" of NOE's from protein to oligonucleotide resonances.

Longitudinal relaxation rates $(1/T_1)$ were measured by a selective saturation–recovery method (Rosevear et al., 1983). Transverse relaxation rates $(1/T_2)$ were calculated from the line width at half-height $(\Delta\nu)$ by using the relation $1/T_2 = \pi\Delta\nu$.

NOE Data Analysis. The cross-relaxation rate (σ_{AB}) for the transfer of energy to spin A upon irradiation of spin B was calculated by using eq 1, in which $f_A(B)_t$ is the NOE to spin

$$f_A(B)_t = \frac{\sigma_{AB}}{\rho_A}(1 - e^{-\rho_A t}) + \frac{\sigma_{AB}}{\rho_A - c}(e^{-\rho_A t} - e^{-ct}) \quad (1)$$

A upon preirradiation of spin B for time t, ρ_A is the spin–lattice relaxation rate of spin A, and c is the rate constant for saturation of spin B, which accounts for the small lag period before the NOE's begin to build up.

Interproton distances (r_{AB}) were obtained from σ_{AB} by using eq 2, in which the constant $D = (\gamma^4\hbar^2/10)^{1/6} = 62.02$ Å $s^{-1/3}$,

$$r_{AB} = D[f(\tau_r)/\sigma_{AB}]^{1/6} \quad (2)$$

where γ is the proton gyromagnetic ratio. In eq 2, $f(\tau_r)$ is given by

$$f(\tau_r) = \frac{6\tau_r}{1 + 4\omega_I^2\tau_r^2} - \tau_r \quad (3)$$

where ω_I is the Larmor frequency and τ_r is the correlation time.

The value of τ_r was calculated for the deoxynucleoside triphosphates from $\sigma_{H2''\rightarrow H1'}$ with eq 2 and the conformationally independent distance of 2.37 ± 0.10 Å between deoxyribose H2″ and deoxyribose H1′. The latter distance is based on model-building and crystallographic studies (Levitt & Warshel, 1978). The values of τ_r for AMPCPP and for oligo$(rA)_{50\pm13}$ were calculated from $\sigma_{H2'\rightarrow H1'}$ with eq 2 and the conformationally insensitive distance of 2.9 ± 0.2 Å (Rosevear et al., 1983). The available X-ray structures of adenosine (Lai & Marsh, 1972) and AMP (Neidle et al., 1976) and the neutron diffraction based structure of 5-nitrouridine (Takusagawa et al., 1979) yield H2′ to H1′ distances that fall within this range. The value of τ_r was calculated for oligo(rU) from $\sigma_{UH6\rightarrow UH5}$ and $\sigma_{UH5\rightarrow UH6}$ and the conformationally independent distance of 2.39 ± 0.15 Å, obtained from the range of distances found

Table I: Kinetic Parameters of Large Fragment of Pol I with Ribonucleotide Templates[a]

template	primer	$K_M^{template}$ (μM)	K_M^{primer} (μM)	K_I(AMPCPP) (μM)	K_M(dATP) (μM)	V_{max} (units/mg)[a]
oligo(rU)$_{46\pm17}$	(Ap)$_9$A	25 ± 10	≤1.8			100 ± 10
poly(rU)	(dA)$_{10}$		≤40			≥150
oligo(rA)$_{50\pm13}$[b]	(dT)$_{10}$	<3.1	<10.5			49 000 ± 5000
oligo(rU)$_{46\pm17}$	(Ap)$_9$A			22 ± 10[c]	47 ± 10[c]	240 ± 24[c]
poly(rU)	(Ap)$_9$A			17 ± 5[d]	130 ± 40[d]	35 ± 5[d,e]

[a] Conditions and components are given under Methods. A unit of enzyme catalyzes the polymerization of 10 nmol of nucleotide in 30 min. [b] The K_M of poly(rA) as template with whole Pol I at 37 °C is significantly lower than 0.4 μM, and the maximal velocity is 6300 units/mg (Travaglini et al., 1975). [c] The K_I of AMPCPP was determined with the following components: oligo(rU)$_{46\pm17}$, 12.8 μM; (Ap)$_9$A, 15.8 μM; dATP, 20–300 μM. [d] The K_I of AMPCPP was determined with the following components: poly(rU), 590 μM in nucleotides; AMPCPP, 0, 15, 30, and 45 μM. All other components and conditions were as described in footnote *c*. [e] Low maximal velocity was due to the low concentration of template (590 μM in nucleotides).

in four independent crystal structures of uracil-containing compounds: uridine (Green et al., 1975), 3′-UMP (Srikrishnan et al., 1979), 2′,3′-*O*-(methoxymethylene)uridine (de Kok et al., 1977), and 3′,5′-diacetyluridine (de Graaff et al., 1977).[2] The upper limit of τ_r was estimated with eq 4 (Solomon, 1955)

$$\frac{T_1}{T_2} = \frac{12\omega_I^4\tau_r^4 + 37\omega_I^2\tau_r^2 + 10}{16\omega_I^2\tau_r^2 + 10} \quad (4)$$

by using the measured T_1/T_2 ratios of the nucleotide protons.

Results and Discussion

Stability of RNA toward the 3′–5′ Exonuclease of the Large Fragment of Pol I. For the reasons stated under Methods, oligoribonucleotides were chosen as templates over blocked oligodeoxyribonucleotides because of their enhanced stability. Even so, partial degradation of the templates in the presence of high concentrations of enzyme was observed. Monophosphate generation could be easily monitored by integration of the aromatic resonances of the mononucleotides that appeared in the NMR spectra such as the U-H6 doublet of 5′-UMP at 8.13 ppm and the A-H8 and A-H2 singlets of AMP at 8.60 and 8.26 ppm, respectively. The amount of degradation differed with the particular enzyme preparation. With one enzyme preparation, oligo(rU)$_{54\pm11}$ was observed to degrade to 5′-UMP at ~2%/h in the presence of Mg^{2+} or ~1%/h in its absence. Oligo(rU)$_{43\pm9}$ degraded at ~4%/h in the presence of Mg^{2+}. Another preparation of enzyme, which had been more thoroughly depleted of whole Pol I, showed a marked decrease in its ability to degrade RNA. Oligo(rU)$_{54\pm11}$ was degraded at a rate of 0.3%/h. Oligo(rA)$_{50\pm13}$ was degraded at a rate of 0.2%/h, with <0.02%/h seen in the absence of Mg^{2+} over a period of 7 days. This might be expected, since the 5′–3′ exonuclease activity found in whole Pol I, but not in the large fragment, has been implicated in the removal of RNA primers during replication in *E. coli* (Westergaard et al., 1973; Ogawa et al., 1977). In all cases, NMR experiments were completed before the extent of degradation of the template or primer exceeded 20%.

Ability of Oligo(rA) and Oligo(rU) To Serve as Templates for the Large Fragments. The ability of RNA to serve as templates for DNA polymerase I is well documented (Karkas et al., 1972; Karkas, 1973; Travaglini et al., 1975). It was noted, however, in these earlier papers that the velocity of polymerization with different polyribonucleotides as templates varied greatly. For this study, it was necessary to show that the oligoribonucleotides under study could in fact serve as templates and to determine their affinity for the template binding site on the large fragment, to ensure that in the NMR experiment the template site would be reasonably well occupied.

Kinetic studies were carried out by varying the template oligo(rU)$_{46\pm17}$ concentration at varying concentrations of the primer (Ap)$_9$A with dATP as substrate. A K_M value of 25 ± 10 μM was obtained for the template at a saturating concentration of primer (41 μM), and a $K_M \leq 1.8$ μM was estimated for the primer on extrapolation to infinite template concentration (Table I). The maximal velocity with oligo(rU)$_{46\pm17}$ as template is 2 orders of magnitude slower than that observed with oligo(rA)$_{50\pm13}$, which, like poly(rA) (Travaglini et al., 1975), is one of the best templates for this enzyme (Table I). The low V_{max} with polyuridylate templates is not due to the ribonucleotide primer since the use of (dA)$_{10}$ with poly(rU) also gives a low value (Table I). Similar low rates of polymerization with poly(rU) as template have been reported by Karkas (1973).[3]

With oligo(rA)$_{50\pm13}$ as template and (dT)$_{10}$ as primer, no change in velocity was observed when the template concentration was varied over the range of 3.1–47 μM, indicating the K_M to be significantly lower than 3.1 μM, as previously found with poly(rA) (Travaglini et al., 1975). Similarly, no change in velocity was observed on lowering the primer concentration from 42 to 10.5 μM, indicating that the system was saturated with primer at the latter concentration.

The high affinity of the enzymes for the ribonucleotide templates detected kinetically ensures that the enzyme will be saturated with template in the NMR experiments. Independent evidence for template binding by the enzyme, obtained by NMR, will be presented in a later section.

Intramolecular Nuclear Overhauser Effects on Enzyme-Bound dATP in the Presence of Oligo(rU)$_{54\pm11}$. The typical 250-MHz proton NMR spectrum of Mg^{2+}dATP (3.4 mM) and the large fragment (0.16 mM) is shown in Figure 1A. Below it (Figure 1B) is shown the spectrum of the complex after the addition of oligo(rU)$_{54\pm11}$ (0.16 mM). As was consistently observed after all such additions, the presence of template did not cause large changes in the chemical shifts of the resonances of the substrate (<0.02 ppm), and within experimental error, no further effects on the line widths or the spin–lattice relaxation rates of the substrate were seen, beyond

[2] This method for calculating τ_r assumes it to be invariant for all interproton interactions of a bound nucleotide or oligonucleotide. Although small errors might thereby be introduced (Keepers & James, 1984; Mossefskin & Bolton, 1985), the validity of this assumption was experimentally justified in the case of enzyme-bound TTP, where the correct interproton distance between TH6 and TH5Me (2.80 ± 0.13 Å) was calculated with the τ_r from the H2″ to H1′ interaction (Table III), and in the other cases by the general agreement of the τ_r values of several protons estimated from their T_1/T_2 ratios (Tables II–VI and VIII). In another system, Mg^{2+}ATP bound to a peptide fragment of adenylate kinase, direct measurements of τ_r by the field dependence of σ and ρ showed τ_r to be invariant (Fry et al., 1985).

[3] The low activity of polyuridylate templates may result in part from the formation of triple helices of the structure A_nU_{2n} (Felsenfeld & Miles, 1967). We have obtained evidence by NMR line broadenings and shifts for the formation of such complexes and for their interaction with the enzyme. Further studies of such complexes are in progress.

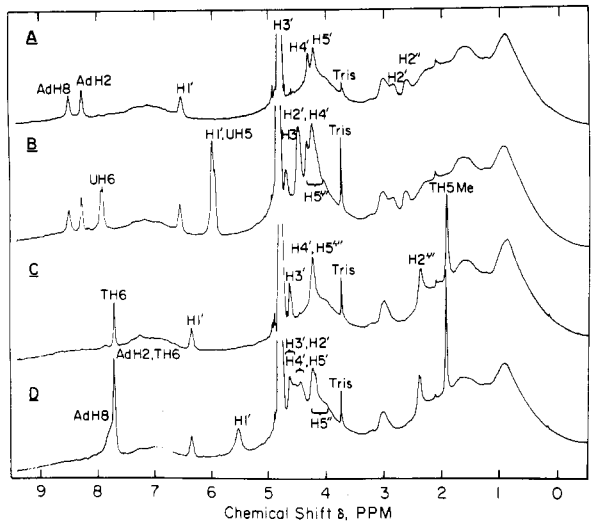

FIGURE 1: Proton NMR spectra of Mg^{2+}dATP and Mg^{2+}TTP in the presence of the large fragment of Pol I and in the absence and presence of the template oligo(rU)$_{54\pm11}$ or oligo(rA)$_{50\pm13}$. (A) is the spectrum of 3.4 mM dATP, 4.5 mM $MgCl_2$, and 0.16 mM large fragment, which was acquired from 64 transients with a recycle time of 7.7 s. (B) is the spectrum of 2.9 mM dATP, 4.3 mM Mg^{2+}, 0.14 mM large fragment, and 0.16 mM oligo(rU). The spectrum was acquired from 512 transients with a recycle time of 2.8 s. (C) is the spectrum of 3.2 mM TTP, 5.2 mM Mg^{2+}, and 0.14 mM large fragment. The spectrum was acquired from 64 transients with a recycle time of 12.7 s. (D) is identical with (C), except that 0.16 mM oligo(rA) was present and a recycle time of 5.7 s was used. All samples contained 10 mM deuterated Tris-HCl buffer, pH* 7.1, and 32 mM KCl in ^2H_2O. T = 24 °C. NMR parameters: 3000-Hz spectral width, 16K time domain points, 16-bit A/D conversion, and 90° flip angle. A line broadening of 0.5 Hz was used.

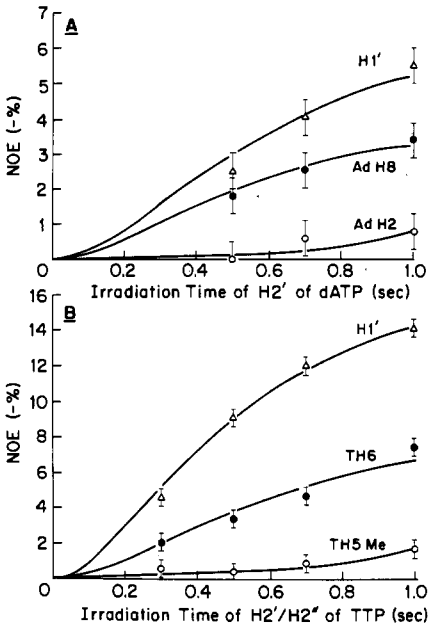

FIGURE 2: Time dependence of NOE's to protons of dATP or TTP after preirradiation of deoxyribose H2′ or H2′/H2″, respectively. Large fragment and either oligo(rU)$_{54\pm11}$ or oligo(rA)$_{50\pm13}$ were present. (A) shows the NOE's to adenine H8, adenine H2, and deoxyribose H1′ of dATP upon preirradiation of deoxyribose H2′. The two upper curves represent theoretical fits to the primary NOE's with eq 1 and the parameters given in Table II. The lower curve represents a secondary NOE from deoxyribose H2′ to adenine H2. The sample contained the following (in mM): dATP, 2.9; Mg^{2+}, 4.3; large fragment, 0.14; oligo(rU)$_{54\pm11}$, 0.16. A recycle time of 2.8 s was used. (B) shows the NOE's to thymine H6, thymine H5 methyl, and deoxyribose H1′ of TTP upon preirradiation of deoxyribose H2′/H2″. The two upper curves represent theoretical fits to the primary NOE's with eq 1 and the parameters given in Table III. The lower curve represents a secondary NOE from deoxyribose H2′/H2″ to thymine H5 methyl. The sample contained the following (in mM): TTP, 3.2; Mg^{2+}, 5.2; large fragment, 0.14; oligo(rA)$_{50\pm13}$, 0.16. A recycle time of 3.1 s was used. A line broadening of 2.0 Hz was used in processing all NMR data. Other conditions were as described in Figure 1.

those caused by the enzyme alone.

Figure 2A shows the time dependence of the NOE's from deoxyribose H2′ to A-H8, A-H2, and deoxyribose H1′ of dATP and their errors, measured in the presence of the large fragment and stoichiometric oligo(rU)$_{54\pm11}$. Several features of this time dependence are very similar to those observed in the absence of template (Ferrin & Mildvan, 1985b). First, the signs of the NOE's are all negative, indicating that the template did not displace the dATP from the enzyme nor did it lower the correlation time τ_r below 7×10^{-10} s (from eq 2). Second, primary NOE's to deoxyribose H1′ and adenine H8 were observed, which appeared much more rapidly than the secondary NOE's to adenine H2. Third, the small initial lags observed in the primary NOE's that result from the time required to saturate the deoxyribose H2′ resonance (approximated by the rate constant c in eq 1) were quite comparable both in the presence and in the absence of template.

To quantitatively evaluate the effects of template on interproton distances of bound dATP, the time dependence of the primary NOE's $[f_A(B)_t]$, as well as the longitudinal relaxation rates (ρ_A) of individual resonances, was measured, and the cross-relaxation rates (σ_{AB}) for various pairs of spins were calculated by using eq 1. For those pairs of spins showing no primary NOE, the noise level of the NOE experiments, typically ±0.5% as estimated by spectral integration, was used to calculate the upper limit values of σ_{AB}.

As can be seen from eq 2, the ratio of any two interproton distances is equal to the inverse sixth root of the ratio of their σ_{AB} values. An absolute interproton distance requires a value for the correlation function, $f(\tau_r)$. For dATP, $f(\tau_r)$ was determined by using the distance between H2″ and H1′, which is 2.37 ± 0.1 Å for all possible deoxyribonucleotide conformations.[2] An upper-limit τ_r was independently calculated from the T_1/T_2 ratios with eq 4. The values for the longitudinal relaxation rates (ρ_A), the cross-relaxation rates (σ_{AB}), τ_r, $f(\tau_r)$, and the interproton distances (r_{AB}) are given in Table II. Comparison of the interproton distances in Table II with those previously determined in the absence of template (Ferrin & Mildvan, 1985b) reveals that the presence of template slightly increased the distance from deoxyribose H2′ to adenine H8 by 0.2 Å and the distance from deoxyribose H3′ to adenine H8 by 0.4 Å, while the other measured distances did not change, within experimental error.

Conformation of Enzyme-Bound dATP. A framework molecular model was constructed for dATP by using the calculated distances of Table II. From this model, the conformation of dATP bound to the large fragment in the presence of template was found to have a glycosidic torsional angle ($\chi = 62 \pm 10°$) that is clearly anti and a C5′–C4′–C3′–O3′ exocyclic torsional angle ($\delta = 90 \pm 10°$) that identifies the sugar pucker as O1′-endo/C3′-endo. The conformation of bound dATP in the presence and the absence of template is depicted in Figure 3 (left). As can be seen, the addition of template led to a very small increase in the glycosidic torsional angle and a slight increase in the amount of C3′-endo character of the sugar pucker. From a conformation diagram, based on X-ray studies of A, B, and Z DNA (Figure 4; Dickerson et al., 1982), it is seen that the conformations of enzyme-bound dATP, both in the absence and in the presence of template, differ greatly from those of nucleotides of A and Z DNA but are like those of B DNA. The small effect of template on the

Table II: Longitudinal Relaxation Rates, Cross-Relaxation Rates, and Interproton Distances for Enzyme-Bound dATP: Effect of Template

	oligo(rU)$_{54\pm11}$ present[a]						oligo-(rU) absent[i]
	expt 1[j]			expt 2[j]			
proton pair (B → A)[b]	ρ_A (s^{-1})[c]	$-\sigma_{AB}$ (s^{-1})[d]	r_{AB} (Å)[e]	ρ_A (s^{-1})[c]	$-\sigma_{AB}$ (s^{-1})[d]	r_{AB} (Å)[e]	r_{AB} (Å)
H2″ → H1′	2.56	0.274	2.37	2.04	0.256	2.37	2.37
H2′ → A-H8	2.86	0.110	2.76	2.86	0.122	2.68	2.57
H3′ → A-H8	2.86	0.080	2.91	2.86	0.082	2.87	2.53
H4′ → H1′	2.56	0.145	2.64				2.68
H2′ → H1′[f]	2.56	0.163	2.58	2.04	0.164	2.55	2.56
H1′ → A-H8	2.86	≤0.021	≥3.64				≥2.93

	expt 1[j]	expt 2[j]
$f(\tau_r)$ (s)[g]	-8.5×10^{-10}	-8.0×10^{-10}
τ_r (s)[g]	1.3×10^{-9}	1.3×10^{-9}
τ_r from A-H8 T_1/T_2 (s)[h]	$\leq 2.7 \times 10^{-9}$	$\leq 2.7 \times 10^{-9}$
τ_r from A-H2 T_1/T_2 (s)[h]	$\leq 2.0 \times 10^{-9}$	$\leq 2.3 \times 10^{-9}$

[a] ρ values were directly measured, and σ values were obtained by fitting time-dependent NOE's to eq 1, with c values ranging from 4 to 5.8 s^{-1}. [b] B refers to the irradiated resonance. A refers to the observed resonance. [c] Errors in ρ_A are typically ±5%. [d] Errors in σ_{AB} are typically ±15%. [e] Errors in ratio of distances (relative distances) are typically ±3%. Errors in absolute distances are typically ±8% or ~0.2 Å. [f] Due to the proximity of H2′ and H2″ resonances resulting in a mixed effect, these calculated distances were not used in determining the conformation. [g] $f(\tau_r)$ calculated from eq 2 assuming an interproton distance between H2″ and H1′ of 2.37 ± 0.10 Å. τ_r calculated from eq 3. [h] Upper limit correlation times (τ_r) determined from T_1/T_2 ratios with eq 4. [i] The average of distances found in three experiments for dATP bound to the large fragment and whole Pol I in the absence of template (Ferrin & Mildvan, 1985b). The errors in ratio of distances (relative distances) are typically ±2%. Errors in absolute distances are typically ±7%. [j] Experiment 1 was done at the following concentrations (mM); large fragment, 0.132; dATP, 2.85; Mg^{2+}, 4.28; oligo(rU)$_{54\pm11}$, 0.155. Experiment 2 was done at the following concentrations (mM): large fragment, 0.116; dATP, 2.54; Mg^{2+}, 3.89; oligo(rU)$_{54\pm11}$, 0.123. Other components and conditions are as described under Methods.

Table III: Longitudinal Relaxation Rates, Cross-Relaxation Rates, and Interproton Distances for Enzyme-Bound TTP: Effect of Template[a]

	oligo(rA)$_{50\pm13}$ present						oligo-(rA) absent[b]
	expt 1			expt 2			
proton pair (B → A)	ρ_A (s^{-1})	$-\sigma_{AB}$ (s^{-1})	r_{AB} (Å)	ρ_A (s^{-1})	$-\sigma_{AB}$ (s^{-1})	r_{AB} (Å)	r_{AB} (Å)
H2″ → H1′	2.70	0.345	2.37	2.23	0.361	2.37	2.37
H2′ → T-H6	2.55	0.209	2.58	2.25	0.218	2.58	2.56
H3′ → T-H6	2.55	0.134	2.77	2.25	0.093	2.97	2.89
H4′ → H1′	2.70	0.100	2.91	2.23	0.100	2.94	2.74
H5′/H5″ → T-H6	2.55	0.081	3.02	2.25	0.073	3.09	2.98
T-H5 Me → T-H6	2.55	0.142	2.75	2.25	0.134	2.80	2.72
T-H6 → T-H5 Me	1.63	0.097	2.93	1.64	0.129	2.81	2.81
H1′ → T-H6	2.55	≤0.071	≥3.08	2.25	≤0.088	≥3.00	≥3.48
H1′ → T-H5 Me	1.63	≤0.023	≥3.72	1.64	≤0.031	≥3.57	≥4.32
T-H6 → H1′	2.70	≤0.074	≥3.06	2.23	≤0.059	≥3.21	≥3.19
T-H5 Me → H1′	2.70	≤0.010	≥4.28	2.23	≤0.011	≥4.24	≥4.32

	expt 1	expt 2
$f(\tau_r)$ (s)	-1.07×10^{-9}	-1.12×10^{-9}
τ_r (s)	1.5×10^{-9}	1.5×10^{-9}
τ_r from T-H6 T_1/T_2 (s)	$\leq 1.8 \times 10^{-9}$	$\leq 1.7 \times 10^{-9}$
τ_r from T-H5 Me T_1/T_2 (s)	$\leq 2.0 \times 10^{-9}$	$\leq 2.0 \times 10^{-9}$

[a] Experiment 1 was done at the following concentrations (mM): large fragment, 0.136; TTP, 3.17 Mg^{2+}, 5.15; oligo(rA)$_{50\pm13}$, 0.156. Experiment 2 was done at the same concentrations, except that the concentration of Mg^{2+} was 3.47 mM. Other components and conditions are as described in Table II. Definitions and errors are as given in Table II. The c values range from 4 to 12 s^{-1}. [b] Distances for TTP bound to the large fragment (Ferrin & Mildvan, 1985b). Errors are as given in Table II.

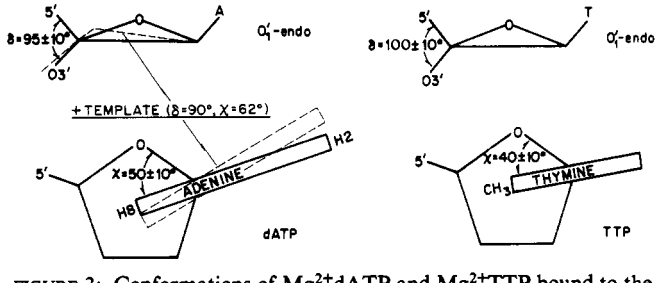

FIGURE 3: Conformations of Mg^{2+}dATP and Mg^{2+}TTP bound to the large fragment of Pol I in the absence (solid lines) and presence (dotted lines) of the templates oligo(rU)$_{54\pm11}$ and oligo(rA)$_{50\pm13}$, respectively. Conformations in the absence of template are taken from a previous publication (Ferrin & Mildvan, 1985b). (Left) Conformation of Mg^{2+}dATP as determined by the distance measurements in Table II. (Right) Conformation of Mg^{2+}TTP as determined by the distances in Table III. The conformations of Mg^{2+}TTP in the presence and absence of template were indistinguishable.

conformation of bound Mg^{2+} dATP is similar to, but not identical with, a result obtained with *E. coli* RNA polymerase by Pillai et al. (1985). Using the paramagnetic effects of Mn^{2+} on the NMR relaxation rates of enzyme-bound ATP, they concluded that the presence of the template poly(dAT) did not alter the conformation of bound Mn^{2+}ATP.

Conformation of Enzyme-Bound TTP in the Presence of the Template Oligo(rA)$_{50\pm13}$. The same conditions and techniques described above were applied to enzyme-bound TTP in the presence of the template oligo(rA)$_{50\pm13}$. Figure 2B shows the time dependence of the intramolecular NOE's from the deoxyribose H2′/H2″ resonances, and their errors, in the presence of the large fragment and a stoichiometric concentration of oligo(rA)$_{50\pm11}$. The complete set of data obtained on eight interproton interactions is given in Table III.

In two of the eight cases, the partial overlapping of both

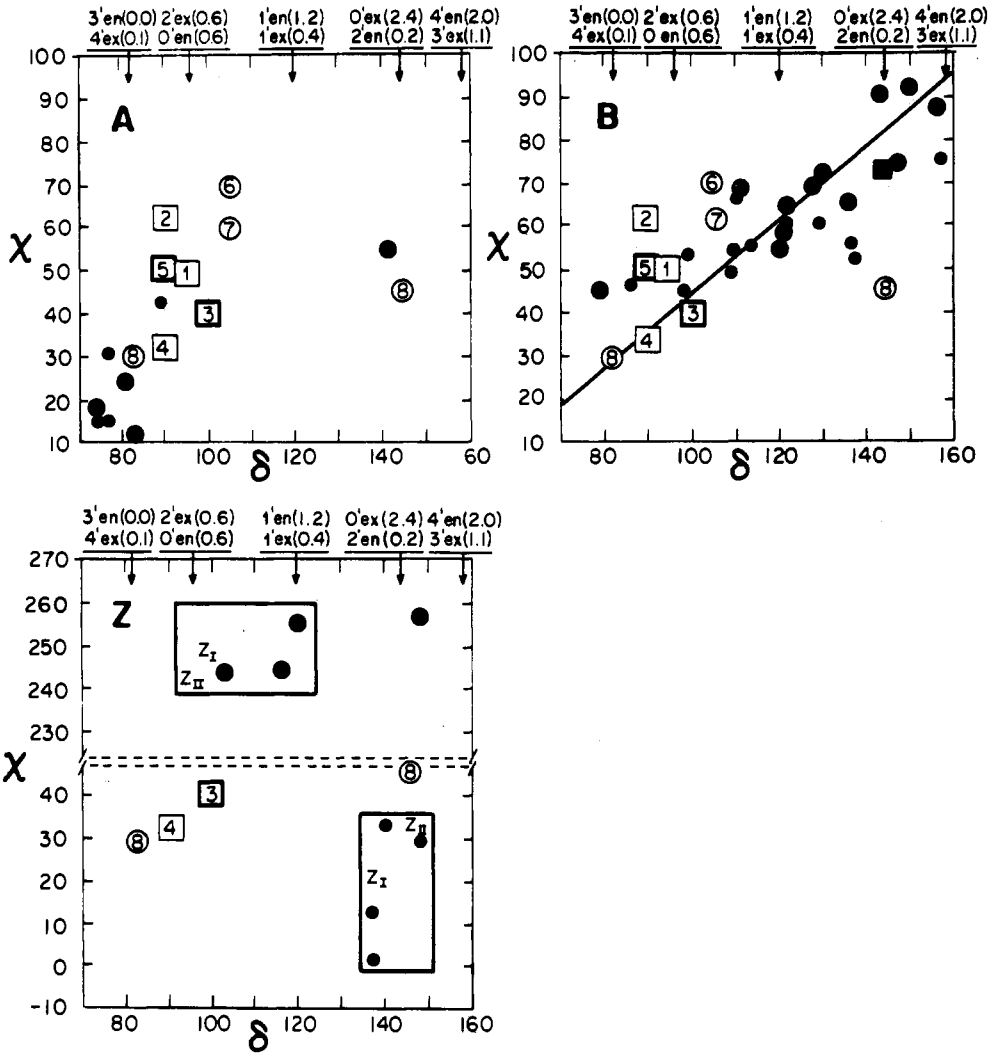

FIGURE 4: Conformation plot of glycosidic torsional angles (χ) vs. deoxyribose C3′–C4′ dihedral angles (δ) in A, B, and Z DNA determined crystallographically (filled symbols) and of several bound nucleoside triphosphate and template nucleotides discussed in the text (open symbols). The diagrams are modified from a review by Dickerson et al. (1982). (A) Dihedral angles found in the A-DNA tetramer CCGG; (B) angles found in the B-DNA dodecamer CGCGAATTCGCG; (Z) angles found in the high-salt Z-DNA tetramer CGCG. The solid line (B) shows the linear correlation between χ and δ characteristic of B DNA. The numbered boxes (substrates) and circles (template nucleotides) correspond to the following structures determined by NMR: (1) dATP in absence of template (Ferrin & Mildvan, 1985b); (2) dATP in presence of template oligo(rU)$_{54\pm11}$; (3) TTP in the absence or presence of template oligo(rA)$_{50\pm13}$; (4) dGTP in the presence of template oligo(rU)$_{43\pm9}$; (5) AMPCPP in the absence or presence of template or template-primer; (6) oligo(rU)$_{54\pm11}$ in the absence of enzyme; (7) oligo(rU)$_{54\pm11}$ in the presence of enzyme; (8) oligo(rA)$_{50\pm13}$ in the presence of enzyme. (Two alternatives are shown.)

the irradiated and observed resonances of TTP with those of oligo(rA)$_{50\pm13}$ (Figure 1D) required additional control experiments to accurately evaluate the intramolecular NOE's of bound TTP. Thus, the overlap of the T-H6 resonance of Mg^{2+}TTP with that of A-H2 of oligo(rA)$_{50\pm13}$ and of the deoxyribose H3′, H5′, and H5″ resonances with those of ribose interfered with the measurement of the NOE's from H3′ and H5′/H5″ to T-H6. This complication was dealt with in the following manner: NOE experiments using the pulse durations, powers, and frequencies appropriate for the TTP complex were carried out on the large fragment–oligo(rA)$_{50\pm13}$ complex in the absence of TTP. TTP was then added, and the identical experiments were repeated. The NOE difference spectra in the absence of TTP were then subtracted from the appropriate difference spectra in the presence of TTP. In such a manner, the NOE's from H3′ to TH6 and from H5′/H5″ to TH6 were determined. It is obvious that in such experiments the exact experimental conditions and resonance frequencies must be known beforehand. This method was tested and was shown not to alter the NOE's in cases of nonoverlapping resonances. In six of the eight interproton interactions of Table III, this procedure was found not to be necessary. On the basis of the interproton distances (Table III), the molecular model built for enzyme-bound TTP in the presence of oligo(rA)$_{50\pm13}$ [Figure 3 (right)] had an anti-glycosidic torsional angle, χ, of 40 ± 10° and an O1′-endo pucker with δ = 100 ± 10°. This structure, which is indistinguishable from that obtained in the absence of template (Ferrin & Mildvan, 1985b), is compatible with B DNA but not with A or Z DNA (Figure 4).

Conformation of Enzyme-Bound dGTP in the Presence and Absence of Template Oligo(rU)$_{43\pm9}$. The same conditions and techniques used above were applied to enzyme-bound dGTP. The interproton distances obtained are given in Table IV. The conformation of dGTP found in the presence of oligo(rU) will be discussed first since it is simpler. The molecular model constructed for bound dGTP in the presence of oligo(rU)$_{43\pm9}$ (Figure 5) was found to have an anti-glycosidic torsional angle, χ, of 32 ± 10° and an O1′-endo/C3′-endo deoxyribose pucker with δ = 90 ± 10°. This conformation fits well onto the correlation of δ with χ found for the nucleotides of B DNA but lies between the B and the A conformations.

When the above procedure was applied to enzyme-bound

Table IV: Longitudinal Relaxation Rates, Cross-Relaxation Rates, and Interproton Distances for Enzyme-Bound dGTP: Effect of Template[a]

proton pair (B → A)	oligo(rU)$_{43\pm9}$ present			oligo(rU) absent		
	ρ_A (s^{-1})	$-\sigma_{AB}$ (s^{-1})	r_{AB} (Å)	ρ_A (s^{-1})	$-\sigma_{AB}$ (s^{-1})	r_{AB} (Å)
H2 → H1′	2.16	0.293	2.37	2.62	0.259	2.37
H2′ → G-H8	2.99	0.185	2.56	2.92	0.104	2.76
H3′ → G-H8	2.99	0.152	2.64	2.92	0.114	2.72
H5′/H5″ → G-H8				2.92	0.093	2.81
H4′ → H1′	2.16	0.102	2.83	2.62	0.109	2.74
H1′ → G-H8	2.99	0.033	3.41	2.92	0.105	2.75
G-H8 → H1′				2.62	0.143	2.62

	oligo(rU)$_{43\pm9}$	oligo(rU) absent
$f(\tau_r)$ (s)	-9.1×10^{-10}	-8.1×10^{-10}
τ_r (s)	1.3×10^{-9}	1.3×10^{-9}
τ_r from G-H8 T_1/T_2 (s)	$\leq 1.6 \times 10^{-9}$	$\leq 1.7 \times 10^{-9}$

[a] The experiments were done at the following concentrations (mM): large fragment, 0.154; dGTP, 3.35; Mg^{2+}, 4.50; oligo(rU)$_{43\pm9}$, 0.190 when present. Other components and conditions are as described in Table II. Definitions and errors are as described in Table II. A c value of 5 s^{-1} was used.

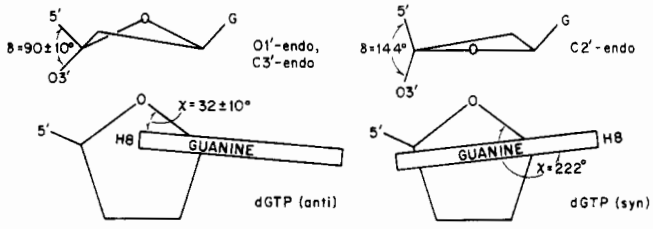

FIGURE 5: Conformations of Mg^{2+}dGTP bound to the large fragment in the presence and absence of the template oligo(rU)$_{43\pm9}$. (Left) The anti conformation of Mg^{2+}dGTP in the presence of template as determined by the distances in Table IV. (Right) The syn conformation of deoxyguanosine as determined by Hashemeyer and Sobell (1965). A 40 ± 5% contribution of this conformation in addition to an anti conformation was necessary to account for the distances observed with enzyme-bound Mg^{2+}dGTP in the absence of template (Table IV).

dGTP in the absence of template, the interproton distances obtained (Table IV) differed from those found in the presence of template (Table IV). Most significantly, the measured distance between deoxyribose H1′ and guanosine H8 decreased by 0.7 Å when no oligo(rU) template was present. Moreover, the distances obtained in the absence of template were not consistent with any single conformation of dGTP, indicating that more than one conformation of the bound nucleotide, including both syn and anti forms, was necessary to fit the NOE data. Similar observations were made by Rosevear et al. (1983) on free $Co(NH_3)_4ATP$ in solution, which required at least three conformations to explain the interproton distances. In the present case, it is clear that enzyme-bound dGTP is being observed, since the NOE's are all negative and arise rapidly. It is also clear from binding studies (Ferrin & Mildvan, 1985b) that dGTP occupies only one site per enzyme molecule under these conditions.

The method of Rosevear et al. (1983), using established conformations of deoxyguanosine as a basis set, was used to estimate the fractional contribution of each conformation to the observed average. The simplest fit to the average distances of Table IV was obtained by assuming a 60 ± 5% contribution of the anti conformation found for dGTP in the presence of oligo(rU)$_{43\pm9}$ as described above and a 40 ± 5% contribution from a structure with a syn torsional angle (χ = 222°) and a C2′-endo deoxyribose pucker (δ = 144°), as has been found in the X-ray structure of deoxyguanosine (Haschemeyer & Sobell, 1965). In all fits to the measured distances of Table IV, a 40 ± 5% contribution of this syn conformation was found to be necessary. An alternative syn conformation with χ = 222° and an O1′-endo/C3′-endo deoxyribose pucker would also fit the data. However, to our knowledge, no such structure has been found by X-ray.

Within experimental error, alternative anti conformations could be used to satisfy the 60 ± 5% anti contribution to the average. Thus, the anti contribution could be provided by the conformation found for enzyme-bound dATP in the absence of template (χ = 50 ± 10°), O1′-endo/C3′-endo deoxyribose pucker (δ = 95 ± 10°) (Ferrin & Mildvan, 1985b), or by a mixture consisting of 40 ± 5% of the conformation found by X-ray for dGMP (χ = 57°), O1′-endo/C4′-exo, (δ = 93°) (Young et al., 1974), and of 20 ± 5% of that found for the deoxyguanosine portion of a dCpG–proflavin complex (χ = 80°), C3′-endo (δ = 94°) (Shieh et al., 1980). On the basis of the data and their errors in Table IV, a choice between the above possibilities could not be made, but in every case, a 40 ± 5% contribution from a structure with a syn-glycosidic torsional angle was necessary. It is of interest that the presence of the template oligo(rU)$_{43\pm9}$ significantly altered the conformation of bound dGTP and simplified it to a single anti species. This change may result from hydrogen bonding between the bound guanine and uracil rings as in the well-known G-U wobble base pair in yeast $tRNA^{Phe}$ (Rich & Raj Bhandary, 1976). Despite this possibility, we will show in a later section that no excessive amount of misincorporation of guanine residues occurs with this enzyme when oligo(rU) is used as the template.

Active Site Binding of AMPCPP. In order to avoid a polymerization reaction in an otherwise complete system to be used for NMR studies, the unreactive substrate analogue AMPCPP was used. In kinetic studies with poly(rU) as template and $(Ap)_9A$ as primer, AMPCPP was found to be a linear competitive inhibitor, with respect to the substrate dATP, with a K_I of 17 ± 5 μM (Table I). Similarly, with oligo(rU)$_{46\pm17}$ as template, under otherwise identical conditions, AMPCPP was a competitive inhibitor against dATP with a K_I of 22 ± 10 μM (Table I). These values are comparable to or even lower than the K_M of dATP, indicating the tight binding of AMPCPP at the active site of the enzyme.

We have previously shown, by intermolecular NOE's from the enzyme to dATP and TTP, that these substrates bind to the large fragment of Pol I near two hydrophobic residues, at least one of which is Ile, and near an unidentified aromatic residue (Ferrin & Mildvan, 1985b). As a further test of the binding of AMPCPP to the substrate site, NOE's were sought from the enzyme (0.14 mM) to the protons of this analogue (3.1 mM). Preirradiation for 1 s in the aliphatic region of the enzyme from 0.6 to 1.8 ppm produced intermolecular NOE's to A-H8, A-H2, and ribose H1′ of AMPCPP similar in

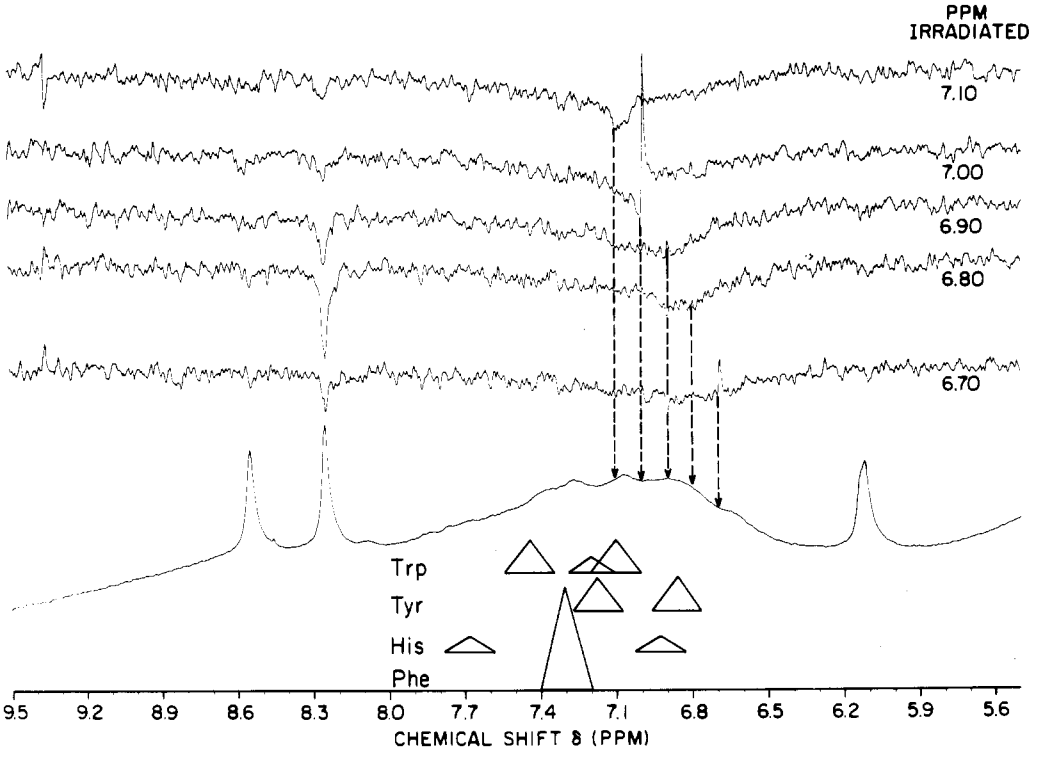

FIGURE 6: Intermolecular NOE's from the large fragment of Pol I to protons of Mg^{2+}AMPCPP, as a function of preirradiation frequency. A control spectrum of enzyme (0.14 mM), Mg^{2+} (4.1 mM), and AMPCPP (3.1 mM) is shown as are the approximate chemical shifts and line widths of the aromatic amino acids. The preirradiation times were 0.5 s. Other conditions are as described in Figures 1 and 2.

Table V: Effects of Template and Primer on Relaxation Rates and Interproton Distances for Enzyme-Bound AMPCPP[a]

	with large fragment only			+template			+template-primer		
proton pair (B → A)	ρ_A (s^{-1})	$-\sigma_{AB}$ (s^{-1})	r_{AB} (Å)	ρ_A (s^{-1})	$-\sigma_{AB}$ (s^{-1})	r_{AB} (Å)	ρ_A (s^{-1})	$-\sigma_{AB}$ (s^{-1})	r_{AB} (Å)
H2′ → H1′	1.30	0.181	2.90	1.35	0.197	2.90	1.42	0.192	2.90
H2′ → A-H8	2.90	0.168	2.94	2.65	0.163	2.99	3.14	0.163	2.98
H3′ → A-H8	2.90	0.316	2.64	2.65	0.290	2.72	3.14	0.309	2.68
H5′/H5″ → A-H8	2.90	0.088	3.27	2.65	0.085	3.34	3.14	0.101	3.23
H4′ → H1′	1.30	0.098	3.21	1.35	0.105	3.22	1.42	0.094	3.27
H1′ → A-H8	2.90	≤0.061	≥3.48	2.65	≤0.072	≥3.43	3.14	≤0.075	≥3.39
A-H8 → H1′	1.30	≤0.055	≥3.54	1.35	≤0.069	≥3.45	1.42	≤0.055	≥3.57
H5′/H5″ → A-H2	0.88	≤0.016	≥4.35	0.88	≤0.016	≥4.41			
H5′/H5″ → α,β-CH_2	1.97	≤0.055	≥3.54						
A-H8 → α,β-CH_2	1.97	≤0.042	≥3.70						
H3′ → α,β-CH_2	1.97	≤0.033	≥3.85						

	with large fragment only	+template	+template-primer
$f(\tau_r)$ (s)	-1.9×10^{-9}	-2.1×10^{-9}	-2.0×10^{-9}
τ_r (s)	2.2×10^{-9}	2.3×10^{-9}	2.3×10^{-9}
τ_r from A-H8 T_1/T_2 (s)	$\leq 1.7 \times 10^{-9}$	$\leq 2.0 \times 10^{-9}$	$\leq 1.7 \times 10^{-9}$
τ_r from A-H2 T_1/T_2 (s)	$\leq 3.0 \times 10^{-9}$	$\leq 3.5 \times 10^{-9}$	
τ_r from H1′ T_1/T_2 (s)	$\leq 2.6 \times 10^{-9}$	$\leq 2.5 \times 10^{-9}$	$\leq 2.5 \times 10^{-9}$

[a] All experiments were done at the following concentrations (mM): large fragment, 0.14; AMPCPP, 3.1; Mg^{2+}, 4.1. In addition, the experiment with template oligo$(rU)_{54\pm11}$ contained 0.17 mM template, and the subsequent experiment with template-primer contained an additional 0.19 mM of the primer $(Ap)_9A$. c values ranged from 4 to 10 s^{-1}. All other components and conditions are as described in Table II.

magnitude and chemical shift to those found with dATP, establishing the proximity of hydrophobic amino acids to bound AMPCPP. Much stronger NOE's were also detected from the aromatic region of the enzyme to A-H2 of AMPCPP, establishing the proximity of an aromatic residue to the bound analogue. A detailed action spectrum of the aromatic region, obtained by preirradiation of the proton resonances of the enzyme for 0.5 s (Figure 6), revealed a maximal NOE from a resonance at 6.8 ppm consistent with the proximity of the ortho protons of a tyrosine residue to A-H2 of the bound analogue. A less likely possibility, which cannot yet be excluded, is a histidine C4 proton. A tyrosine residue would be consistent with the results of recent photoaffinity labeling with 8-azido-dATP, which labels Tyr-766 in the Pol I sequence (Joyce et al., 1985b). The addition of the template oligo$(rU)_{54\pm11}$ produced a very small downfield shift in the peak of the action spectrum to 6.9 ppm, possibly due to an aromatic edge effect on the residue from either the template or the substrate analogue. Hence, the analogue AMPCPP, like the substrates dATP and TTP, binds near both hydrophobic and an aromatic amino acid, which appears to be a tyrosine residue. The ~3-fold greater magnitude of the NOE from this residue to A-H2 of the analogue than to dATP (Ferrin & Mildvan, 1985b) suggests that this amino acid is ~20% closer to A-H2 of AMPCPP than to A-H2 of dATP.

Effect of Template and Primer on Conformation of Enzyme-Bound AMPCPP. Table V summarizes the longitudinal and cross-relaxation rates and the interproton distances in

AMPCPP bound to the large fragment of Pol I. A model of bound AMPCPP based on the interproton distances yielded a high anti conformation (χ = 50 ± 10°) with an O1′-endo/C3′-endo ribose pucker (δ = 90 ± 10°). These parameters are very similar to those of enzyme-bound dATP and are therefore more like the nucleotides of B DNA than of A or Z DNA (Figures 3 and 4) (Ferrin & Mildvan, 1985b). The binding of the template oligo(rU)$_{54\pm11}$ and the subsequent binding of the primer (Ap)$_9$A to the enzyme did not alter the interproton distances in enzyme-bound AMPCPP (Table V). Hence, the template and primer induced no further change in the conformation of AMPCPP over that produced by the enzyme alone.

Mutual Displacement of Deoxynucleoside Triphosphate Substrates from the Enzyme in the Presence of Template and Template-Primer. Pol I is known to bind deoxynucleoside triphosphate substrates competitively at a single site in the absence of template and in the presence of Mg^{2+}, as determined by equilibrium dialysis (Englund et al., 1969a). Similar substrate binding properties and affinities were found for the large fragment of Pol I by NMR titrations, measuring the broadening of substrate resonances induced by the enzyme and the renarrowing of these resonances on displacement of one substrate by a second one (Ferrin & Mildvan, 1985b). The dissociation constants of substrates from the large fragment of Pol I, in the absence of template but in the presence of Mg^{2+}, were found to be in the ratio 1.00:5 ± 3:5.5 ± 1.5 for dGTP:dATP:TTP, respectively. Similar NMR titrations were carried out in the presence of templates or of template-primer (Figure 7). Interestingly, the displacement of dATP from the enzyme–oligo(rU)$_{54\pm11}$–Mg^{2+} dATP complex by Mg^{2+}-dGTP (Figure 7A) yielded a K_D(dATP)/K_D(dGTP) of 5.0 ± 1.5 indistinguishable from that found without the template. In the presence of both the template oligo(rU)$_{54\pm11}$ and the primer (Ap)$_9$A, the K_D(AMPCPP)/K_D(dGTP) ratio was found to be 1.5 ± 0.5 (Figure 7C), again indicating no unusual binding preference for the correct (adenine) nucleotide over the incorrect (guanine) nucleotide. Because of the possible formation of a "wobble" G-U base pair on the enzyme, a displacement titration of TTP from the enzyme–oligo(rA)$_{50\pm13}$–Mg^{2+}TTP complex by Mg^{2+}dGTP was carried out (Figure 7B). Again, a K_D(TTP)/K_D(dGTP) of only 3.0 ± 1.0 was found, which overlaps with the value of 5.5 ± 1.5 found in the absence of template (Ferrin & Mildvan, 1985b).

A study of the misincorporation of deoxyguanosine nucleotides into DNA with oligo(rU)$_{54\pm11}$ (11 μM) as template, oligo(dA)$_{10}$ (11 μM) as primer, and equal concentrations of dATP and dGTP (100 μM) yielded a misincorporation rate of $\leq 4 \times 10^{-5}$ guanines per adenine. Hence, the ribonucleotide template oligo(rU) is copied by the large fragment with extremely high fidelity, which is typical of Pol I (Loeb & Kunkel, 1982).

Suggested Mechanism of Substrate Incorporation by Pol I. As shown by the NMR titrations (Figure 7), the presence of templates or of the template-primer did not selectively raise the affinity of the enzyme for the correct nucleotide, nor did they selectively lower the affinity of the enzyme for the incorrect nucleotide. This observation, which was previously made on the basis of steady-state kinetic studies of Pol I (Travaglini et al., 1975), indicates that a step following the binding of the substrate must be responsible for the unusually high fidelity of template copying by DNA polymerase I and its large fragment. As discussed in detail elsewhere (Mildvan & Loeb, 1979; Loeb & Kunkel, 1982), Pol I improves on the fidelity expected from Watson–Crick base pairing alone by

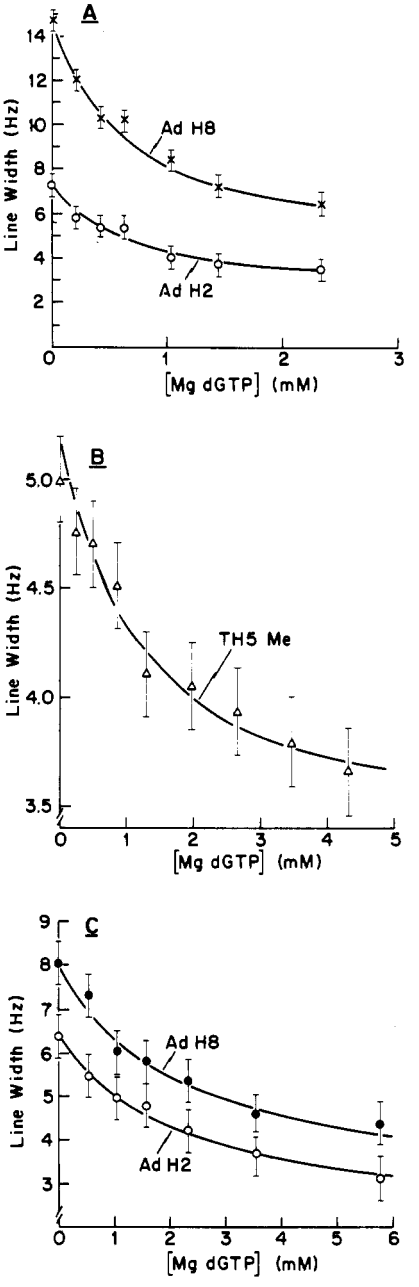

FIGURE 7: Effect of Mg^{2+}dGTP on diamagnetic line broadening of resonances of Mg^{2+}dATP, Mg^{2+}TTP, and Mg^{2+}AMPCPP in the presence of oligo(rU)$_{54\pm11}$, oligo(rA)$_{50\pm13}$, or oligo(rU)$_{54\pm11}$–(Ap)$_9$A, respectively. Samples of Mg^{2+}dATP, Mg^{2+}TTP, or Mg^{2+}AMPCPP in the presence of the large fragment and above template or template-primer were titrated with concentrated solutions of Mg^{2+}dGTP. The line widths, measured at half-height, were plotted as a function of the concentration of Mg^{2+}dGTP. The solid lines were calculated as described in Ferrin and Mildvan (1985b) by assuming competitive binding at a single site on the large fragment with the relative K_D's listed in the text. (A) Effect of Mg^{2+}dGTP on the line widths of Mg^{2+}dATP. The experiment was done at the following concentrations (mM): dATP, 2.8; large fragment, 0.13; oligo(rU)$_{54\pm11}$, 0.17; Mg^{2+}, 1.5 in excess of nucleotide. The spectra were acquired with 64 transients with a recycle time of 7.7 s. (B) Effect of Mg^{2+}dGTP on the line widths of Mg^{2+}TTP. The experiment was done at the following concentrations (mM): TTP, 3.2; large fragment, 0.14; oligo(rA)$_{50\pm13}$, 0.16; Mg^{2+}, 2.0 in excess of nucleotide. The spectra were acquired with 64 transients with a recycle time of 7.7 s. (C) Effect of Mg^{2+}dGTP on the line widths of Mg^{2+}AMPCPP. The experiment was done at the following concentrations (mM): AMPCPP, 3.1; large fragment, 0.14; oligo(rU)$_{54\pm11}$, 0.17; (Ap)$_9$A, 0.19; Mg^{2+}, 1.0 in excess of nucleotide. The spectra were acquired from 128 transients with a recycle time of 10.0 s. All other experimental and NMR parameters were as described in Figure 1.

Table VI: Relaxation Rates and Interproton Distances for Free and Enzyme-Bound Oligo(rU)$_{54\pm11}$[a]

	free			bound		
proton pair (B → A)	ρ_A (s^{-1})	$-\sigma_{AB}$ (s^{-1})	r_{AB} (Å)	ρ_A (s^{-1})	$-\sigma_{AB}$ (s^{-1})	r_{AB} (Å)
U-H6 → U-H5	1.43	0.069	2.47	1.32	1.23	2.41
U-H5 → U-H6	2.44	0.101	2.32	3.28	1.32	2.38
H2′ → U-H6	2.44	0.109	2.29	3.28	0.82	2.57
H2′/H4′ → H1′	1.01	0.059	3.18/2.65[b]	1.32	0.90	3.18/2.65[b]
H3′ → U-H6	2.44	≤0.036	≥2.76	3.28	≤0.17	≥3.35
U-H6 → H1′	1.01	≤0.015	≥3.19	1.32	≤0.16	≥3.38

	free	bound
$f(\tau_r)$ (s)	-0.28×10^{-9}	-4.2×10^{-9}
τ_r (s)	0.9×10^{-9}	4.3×10^{-9}
τ_r from T_1/T_2 of U-H6 (s)	$\leq 1.2 \times 10^{-9}$	2.5×10^{-9}
$1/T_2$ of U-H6 (s^{-1})	10.5	43.4

[a] The experiment done with free oligo(rU)$_{54\pm11}$ was done at the following concentrations (mM): oligo(rU)$_{54\pm11}$, 0.078; Mg^{2+}, 0.96. The experiment done on enzyme-bound oligo(rU)$_{54\pm11}$ was done at the following concentrations (mM): oligo(rU)$_{54\pm11}$, 0.125; large fragment, 0.139. Other conditions and components are as given in Table II. Definitions and errors are as given in Table II. c values of 10 and 20 s^{-1} were used for free and bound oligo(rU)$_{54\pm11}$, respectively. [b] Because of overlap of the H2′ and H4′ resonances, the distances were calculated by assuming the summation of σ values from both H2′ and H4′ to H1′. From the structural studies of Levitt and Warshel (1978), the large cross-relaxation rate observed can result only from an O1′-endo ribose pucker. Model building based on these distances yielded a δ angle of 105°.

a factor of ~10^4. Since the excision of incorrectly incorporated nucleotides by Pol I contributes only 1 of these 4 orders of magnitude to the fidelity of Pol I (Kunkel et al., 1981), such proofreading plays a relatively minor role. Hence, an error prevention or verification step is needed, which follows the binding of the substrate and precedes the primer elongation step. Evidence for such an additional and rate-limiting step in the DNA polymerase reaction has recently been detected by rapid-quench kinetics, but the chemical nature of this rate-limiting step is not clear (Bryant et al., 1983; Mizrahi et al., 1985).

We have suggested a chemical mechanism for this two-step process (Ferrin et al., 1986). In the first step, the substrate binds to the enzyme and interacts with the enzyme-bound divalent cation only via its γ-phosphoryl group as was found by NMR in the abortive Pol I–Mn^{2+}TTP complex (Sloan et al., 1975). In the second or verification step, only if a proper Watson–Crick base pair, but not a wobble base pair, can form between the substrate and the template, the β-phosphoryl group of the substrate also coordinates to the enzyme-bound metal. Such β-coordination has been detected kinetically in the active complex of Pol I by the loss of chiral preference for β-thioTTP on changing the metal activator from Mg^{2+} to Co^{2+} (Burgers & Eckstein, 1979). The coordination of the β-phosphoryl group would close the six-membered chelate ring, thereby further activating the departure of the pyrophosphate leaving group. Moreover, as shown by model-building studies based on the conformations of the enzyme-bound substrates (Sloan et al., 1975; Ferrin & Mildvan, 1985b; Ferrin et al., 1986), β-coordination would decrease the reaction coordinate distance between the entering 3′-OH group of the primer terminus and the α-phosphorus of the substrate from 6 Å in the monodentate complex to 4 Å in the chelate (Ferrin et al., 1986), a value appropriate for an associative nucleophilic substitution on phosphorus (Mildvan, 1981). If such base pairing and coordination of the β-phosphoryl group were significantly slower than the prior equilibration of the substrate with the enzyme, as suggested by the rapid-quench studies (Bryant et al., 1983), then little effect on the relative affinities of the enzyme for the correct and incorrect substrates would be expected in binding studies, as we observe.

Effects of the Large Fragment of Pol I on NMR Parameters of Oligo(rU)$_{54\pm11}$. A comparison of the NMR spectra of oligo(rU)$_{54\pm11}$ in the absence and presence of a comparable amount of enzyme (Figure 8) provides direct evidence for oligonucleotide binding. Thus, the enzyme broadens the proton

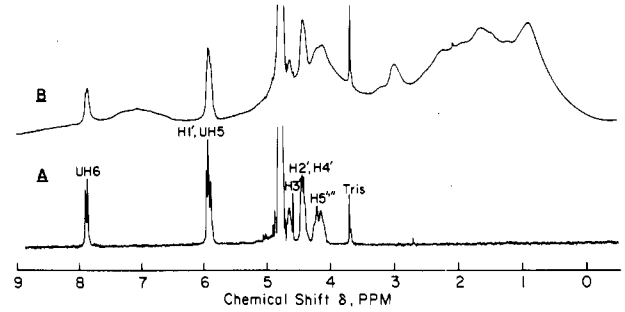

FIGURE 8: Effect of large fragment of Pol I on proton NMR spectrum of oligo(rU)$_{54\pm11}$. Spectrum A is of 0.078 mM oligo(rU)$_{54\pm11}$. Spectrum B is of 0.125 mM oligo(rU)$_{54\pm11}$ in the presence of 0.139 mM large fragment of Pol I. Other components and conditions are as described in Figure 1.

resonances of the oligonucleotide but does not alter the chemical shifts. In other experiments it was found that these effects were observed independently of the presence of Mg^{2+}. In addition to the effects on $1/T_2$, the enzyme produced smaller increases in the longitudinal relaxation rates (ρ_A) of some of the proton resonances of (rU)$_{54\pm11}$ (Table VI). The increase in relaxation rates results from a slowed tumbling of the oligonucleotide when bound to the enzyme. An estimate of the correlation time τ_r from the T_1/T_2 ratio of U-H6, which is the most clearly resolved resonance, shows a 2-fold increase in τ_r in the presence of enzyme (Table VI).

Nuclear Overhauser effects and cross-relaxation rates, σ_{AB}, were measured for the proton resonances of oligo(rU)$_{54\pm11}$ in the absence and presence of a stoichiometric amount of enzyme. Examples of the time dependence of the NOE's are shown in Figure 9A. The σ values for U-H6 → U-H5 and for U-H5 → U-H6 were used, together with the known distance between these protons of 2.39 ± 0.15 Å based on X-ray data (see Methods) to calculate the correlation time. These values of τ_r are similar to those obtained by the T_1/T_2 ratio and reveal a 4-fold increase in τ_r in the presence of the enzyme (Table VI), indicative of a partial immobilization of (rU)$_{54\pm11}$ by the enzyme. From these τ_r values, other interproton distances on free and enzyme-bound (rU)$_{54\pm11}$ were determined. As may be seen from Table VI, with the possible exception of the H2′ → U-H6 distance, no significant changes in interproton distances occurred on binding of oligo(rU)$_{54\pm11}$ to the enzyme. Models of the average nucleotidyl unit based on these distances revealed anti conformations with χ values of 70 ± 10° and 60 ± 10°, respectively, for the free and en-

Table VII: Effects of Enzyme and Mg^{2+} on Chemical Shifts and Line Widths in NMR Spectrum of Oligo(rA)$_{50\pm13}$[a]

resonance	δ (ppm) −Mg^{2+} −Enz	δ (ppm) −Mg^{2+} +Enz	δ (ppm) +Mg^{2+} −Enz	δ (ppm) +Mg^{2+} +Enz	Δδ (by Enz) (ppm) −Mg^{2+}	Δδ (by Enz) (ppm) +Mg^{2+}	Δδ (by Mg^{2+}) (ppm) −Enz	Δδ (by Mg^{2+}) (ppm) +Enz	Δδ (calcd) (ppm) (B DNA → A DNA)[b]	line width (Hz) −Mg^{2+} −Enz	line width (Hz) −Mg^{2+} +Enz	line width (Hz) +Mg^{2+} −Enz	line width (Hz) +Mg^{2+} +Enz	Δ line width (Hz) by enzyme −Mg^{2+}	Δ line width (Hz) by enzyme +Mg^{2+}	Δ line width (Hz) by Mg^{2+} −Enz	Δ line width (Hz) by Mg^{2+} +Enz
A-H8	7.75	7.85	7.70	7.85, 7.77[c]	0.10	0.07, 0.15[c]	−0.05	0.00, −0.08[d]	0.56	11.9	21.4	*d*	15.2	9.5	*d*	*d*	−6.2
A-H2	7.68	7.72	7.68	7.73	0.04	0.05	0.00	0.01	0.59	3.4	9.0	7.5	12.7	5.6	5.2	4.1	3.7
H1′	5.48	5.55	5.44	5.55	0.07	0.11	−0.04	0.00		9.0	20.1	13.2	24.7	11.1	11.5	4.2	4.6

[a] From the spectra of Figure 11. [b] From Kan et al. (1982). [c] Two values are given on the basis of the two chemical shifts seen in Figure 11. [d] Not measurable due to multiplicity of chemical shifts.

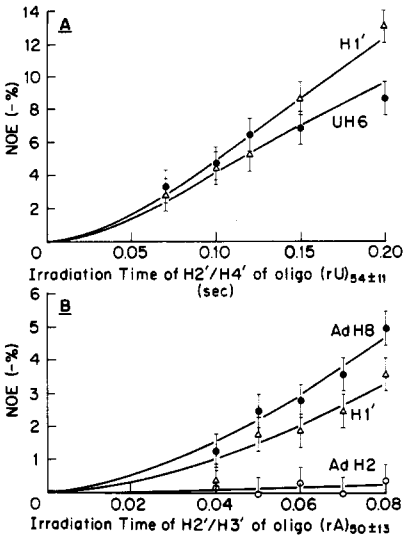

FIGURE 9: Time dependence of NOE's in the presence of enzyme to protons of oligo(rU)$_{54\pm11}$ or oligo(rA)$_{50\pm13}$ after preirradiation of H2′/H4′ or H2′/H3′ resonances, respectively. (A) shows the NOE's to ribose H1′ and uracil H6 upon preirradiation of ribose H2′/H4′. The curves represent theoretical fits to the primary NOE's with eq 1 and the parameters given in Table VI. Concentrations are as given in the legend to Table VI. (B) shows the NOE's to ribose H1′, adenine H8, and adenine H2 upon preirradiation of ribose H2′/H3′. The two upper curves represent theoretical fits to the primary NOE's with eq 1 and the parameters given in Table VIII. The lower curve represents a secondary NOE from ribose H2′/H3′ to H2. Concentrations are as given in the legend to Table VIII.

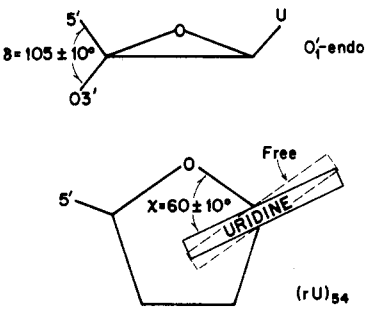

FIGURE 10: Conformation of average uridylate unit of oligo(rU)$_{54\pm11}$ free and bound to the large fragment of Pol I, determined by distance measurements of Table VI.

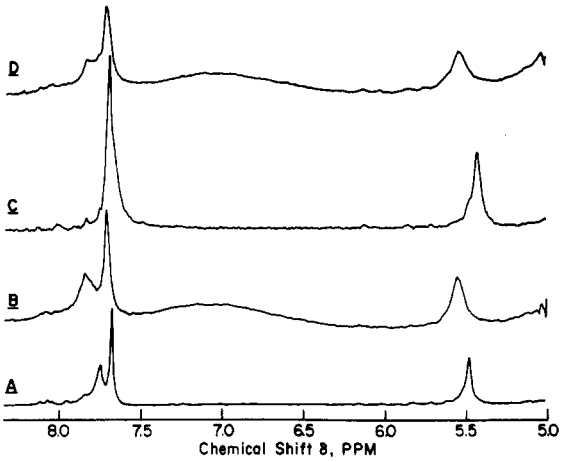

FIGURE 11: Effect of large fragment of Pol I and Mg^{2+} on proton NMR spectrum of oligo(rA)$_{50\pm13}$. (A) is the spectrum of 0.156 mM oligo(rA)$_{50\pm13}$. (B) is that of 0.153 mM (rA)$_{50\pm13}$ in the presence of 0.134 mM enzyme. (C) is that of 0.062 mM oligo(rA)$_{50\pm13}$ with 2.0 mM $MgCl_2$. (D) is that of 0.153 mM oligo(rA)$_{50\pm13}$, 2.0 mM $MgCl_2$, and 0.134 mM large fragment. Other components and conditions are as described in Figure 1.

zyme-bound oligo(rU)$_{54\pm11}$. While the average ribose pucker was not precisely determined, the interproton distances are best fit by an O1′-endo ribose structure ($\delta = 105 \pm 10°$) (Figure 10).

The change in the average χ value induced by enzyme binding is very small (Figure 10), such that the structure of bound (rU)$_{54\pm11}$ remains very near the correlation of χ with δ seen in conformation diagrams of B DNA (Figure 4). As found for the enzyme-bound substrates, the conformation of the average nucleotide of both enzyme-bound and free (rU)$_{54\pm11}$ is neither A- nor Z-like but B-like.

Effects of Enzyme on NMR Parameters of Oligo(rA)$_{50\pm13}$. Figure 11 shows that the enzyme not only broadens but also induces downfield chemical shifts of the A-H8, A-H2, and ribose H1′ resonances of oligo(rA)$_{50\pm13}$. From Table VII, which summarizes the changes in chemical shift and line widths, it is seen that the presence of Mg^{2+} did not greatly alter the effects of the enzyme on these resonances. The addition of Mg^{2+} to oligo(rA)$_{50\pm13}$ in the absence of enzyme caused smaller broadenings and upfield shifts of these resonances. The downfield shifts of the adenine resonances of oligo(rA)$_{50\pm13}$ induced by the enzyme may result from decreases in base stacking as occur in the change in conformation of purine polynucleotides from the A to the B form (Table VII). The effects observed for single-stranded oligo(rA)$_{50\pm13}$ are, however, smaller than those calculated for double-helical polynucleotides. The alternative explanation, that these shifts result from interactions of the purine rings with amino acid residues of the enzyme, is less likely since no shifts of the resonances of oligo(rU)$_{54\pm11}$ were seen. The broadenings of the resonances of oligo(rA)$_{50\pm13}$ induced by the enzyme are due in part to T_2 effects resulting from slowed tumbling, as found for oligo(rU), and also in part to differences in the chemical shifts of the adenine resonances in the enzyme–oligo(rA)$_{50\pm13}$ complex (Figure 11B,D).

Intramolecular NOE's, exemplified in Figure 9B, and T_1 values were measured for enzyme-bound oligo(rA)$_{50\pm13}$ in the

Table VIII: Relaxation Rates and Interproton Distances for Enzyme-Bound Oligo(rA)$_{50\pm13}$[a]

proton pair (B → A)	ρ_A (s^{-1})	$-\sigma_{AB}$ (s^{-1})	r_{AB} (Å)
H2′ → H1′[b]	1.61	0.71	2.90
H2′/H3′ → A-H8[c]	2.99	1.28	2.63
H4′ → H1′	1.61	≤0.58	≥3.00
H5′ → A-H8	2.99	≤0.23	≥3.50
H5″ → A-H8	2.99	≤0.14	≥3.80
A-H8 → H1′	1.61	≤0.29	≥3.37
H1′ → A-H8	2.99	≤0.30	≥3.35
H5′ → A-H2	1.59	≤0.13	≥3.85
H5″ → A-H2	1.59	≤0.13	≥3.85
H2′/H3′ → A-H2	1.59	≤0.072	≥4.25
$f(\tau_r)$ (s)[d]		-7.4×10^{-9}	
τ_r (s)		7.5×10^{-9}	
τ_r from T_1/T_2 of A-H8 (s)		$\leq 3.9 \times 10^{-9}$	
τ_r from T_1/T_2 of A-H2 (s)		$\leq 2.9 \times 10^{-9}$	

[a] The experiment was done at the following concentrations (mM): oligo(rA)$_{50\pm13}$, 0.153; large fragment, 0.134. Other conditions and components are as given in Table II. Definitions and errors are as given in Table II. A c value of 20 s^{-1} was used. [b] Due to an overlap between the H2′ and H3′ resonances, an 18 ± 4% subtraction was applied to the observed cross-relaxation rate between H2′ and H3′ spins and the H1′ spin to obtain a pure value for $\sigma_{H2'\rightarrow H1'}$. For all conformations of ribonucleotides, H2′ is much closer than H3′ to H1′ (Levitt & Warshel, 1978), and the ±4% uncertainty in the $\sigma_{H3'\rightarrow H1'}$ contribution (from eq 2) could result in a maximal error of only ±0.03 Å in the calculated distance between H2′ and H1′. [c] This σ value contains the combined effect of both H2′ → A-H8 and H3′ → A-H8. [d] $f(\tau_r)$ calculated from eq 2 assuming an interproton distance between H2′ and H1′ of 2.90 ± 0.2 Å.

absence of Mg^{2+}, and the resulting cross-relaxation rates were used to calculate average interproton distances, by use of the distance between ribose H2′ and H1′ of 2.9 ± 0.2 Å as an internal standard (Table VIII). The correlation time indicates partial immobilization of the bound oligonucleotide. As determined by model building, the interproton distances are consistent only with an anti conformation for the average adenine nucleotide of bound oligo(rA)$_{50\pm13}$, ruling out the Z conformation. The large distance from H1′ to H4′, exceeding 2.7 Å, rules out the O1′-endo ribose pucker but does not distinguish between C2′-endo and C3′-endo. A more detailed analysis, alternatively assuming either extreme C2′-endo or C3′-endo ribose puckers (Ludemann et al., 1975), yields average χ values of either 45 ± 10° or 30 ± 10°, respectively. The former alternative lies closer to the average nucleotide of B DNA rather than of A DNA. The latter alternative, while in the A-DNA region, lies precisely on the correlation between δ and χ seen in B DNA (Figure 4).

Intermolecular Nuclear Overhauser Effects from Enzyme to Oligo(rU)$_{54\pm11}$ and to Oligo(rA)$_{50\pm13}$. Further evidence for the binding of the oligonucleotide templates to the large fragment of Pol I was obtained by the detection of intermolecular NOE's from protons of the enzyme to those of the templates. Figure 12A shows the NOE action spectrum, resulting from the effects of preirradiation throughout the proton NMR spectrum of the large fragment and observing the intensity of the partially overlapping H1′/U-H5 resonances of oligo(rU)$_{54\pm11}$. In spite of the partial overlap, the large NOE's observed (>1.5%) were mainly to the U-H5 resonance as judged by the chemical shift in the difference spectrum. However, a small additional effect on the ribose H1′ resonance cannot be excluded. No NOE's were observed to the well-resolved U-H6 resonance, and no NOE's were observed upon irradiation in the aromatic region of the enzyme. Such selective effects argue against a significant contribution of nonspecific spin–diffusion to the observed NOE's (Kalk & Berendsen, 1976) and indicate the proximity (i.e., within 5 Å) of several enzyme protons to those of U-H5. The NOE's

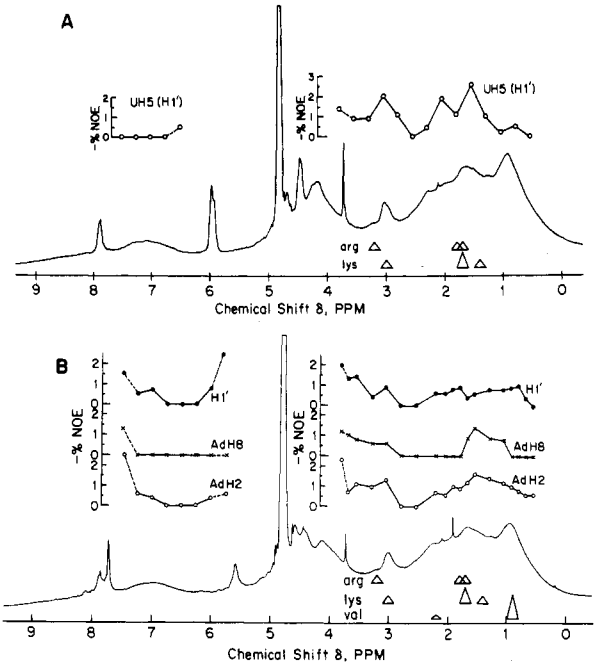

FIGURE 12: NOE action spectra from the large fragment of Pol I to protons of ribonucleotide templates. (A) Action spectrum to oligo(rU)$_{54\pm11}$. The sample contained 0.125 mM oligo(rU)$_{54\pm11}$ and 0.139 mM large fragment. A control spectrum is shown below, as are the approximate chemical shifts and line widths of Arg and Lys protons. (B) Action spectrum to oligo(rA)$_{50\pm13}$. The sample contained 0.153 mM oligo(rA)$_{50\pm13}$ and 0.134 mM large fragment. A control spectrum is shown below, as are the approximate chemical shifts of Arg, Lys, and Val protons. The preirradiation times were 0.5 s. Conditions are otherwise as described in Figures 1 and 2.

observed are most simply explained as arising from irradiation of an Arg or Lys residue of the enzyme (Figure 12A). A number of other residues, however, could contribute partially to the observed effects, as could two or more Arg or Lys residues with similar chemical shifts.

Figure 12B shows the NOE action spectra, resulting from preirradiation throughout the proton NMR spectrum of the large fragment and observing the intensity of the adenine H8 and H2 and ribose H1′ resonances of oligo(rA)$_{50\pm13}$. The results both confirm and extend the observations described above on oligo(rU)$_{54\pm11}$. The presence of Arg or Lys residues near oligo(rA) would explain most of the action spectra. In addition, the NOE's from 0.6 to 0.9 ppm in the protein spectrum to adenine H2 and ribose H1′ argue for the proximity of a hydrophobic residue such as Val, Leu, or Ile to the bound template.

Two independent lines of evidence support the Arg or Lys assignments. First, an amino acid change in *polA6*, a mutant defective in DNA binding (Kelly & Grindley, 1976), has been determined to be a point mutation of Arg-690 to His (Arg-Arg-Ile-Arg → Arg-Arg-Ile-His) (Joyce et al., 1985a). Second, a net positive charge potential in the cleft that has been proposed to be the DNA binding site was calculated, on the basis of the alignment of the amino acid sequence with the X-ray structure of large fragment (Ollis et al., 1985). The interaction of multiple cationic residues with anionic phosphate groups of polynucleotide double helices would explain the high affinity of the enzyme for the template and primer (Englund et al., 1969b).

CONCLUSIONS

The conformations of the substrates dATP and TTP, and of the substrate analogue AMPCPP, bound to the large

fragment of Pol I are similar to those of nucleotides of B DNA and differ greatly from those of A and Z DNA. Templates and primers exert little or no further effects on these conformations. In contrast, enzyme-bound dGTP exists in at least two conformations in the absence of template, while in the presence of oligo(rU)$_{43\pm9}$ only a single B-like conformation is detected. Despite this, guanine deoxynucleotides are not misincorporated by Pol I when oligo(rU) is used as the template. Templates and primer do not alter the relative affinities of the enzyme for complementary and noncomplementary substrates. Hence, a verification step, subsequent to substrate binding and prior to DNA chain elongation, is necessary to explain the high fidelity of template replication by Pol I. Like the substrates, the enzyme-bound oligoribonucleotide templates oligo(rU) and oligo(rA) are partially immobilized and are held in a conformation such that their average nucleotides are more B-like than A- or Z-like. NOE studies indicate that the enzyme binds substrates by using hydrophobic residues, including Ile, and an aromatic residue, probably Tyr. The enzyme binds templates by using cationic Arg and/or Lys residues, and possibly a hydrophobic residue.

ACKNOWLEDGMENTS

We are grateful to Nigel Grindley, Fred Bollum, Barbara Sollner-Webb, David Draper, Larry Loeb, Fritz Eckstein, Jeremy Berg, and Paul Miller for their generous advice and help at various stages of this work.

REFERENCES

Bock, R. M. (1967) *Methods Enzymol. 12*, 218–221.
Bollum, F. J. (1974) *Enzymes (3rd Ed.) 10*, 145–171.
Brutlag, D., & Kornberg, A. (1972) *J. Biol. Chem. 247*, 241–248.
Bryant, F. R., Johnson, K. A., & Benkovic, S. J. (1983) *Biochemistry 22*, 3537–3551.
Burgers, P. M. J., & Eckstein, F. (1979) *J. Biol. Chem. 254*, 6889–6893.
Chatterji, D., Wu, C., & Wu, F. Y.-H. (1984) *J. Biol. Chem. 259*, 284–289.
de Graaff, R. A. G., Admiraal, G., Koen, E. H., & Romers, C. (1977) *Acta Crystallogr., Sect. B: Struct. Crystallogr. Cryst. Chem. B33*, 2459–2464.
de Kok, A. J., Romers, C., de Leeuw, H. P. M., Altona, C., & van Boom, J. H. (1977) *J. Chem. Soc., Perkin Trans. 2*, 487–494.
Dickerson, R. E., Drew, H. R., Conner, B. N., Wing, R. M., Fratini, A. V., & Kopka, M. L. (1982) *Science (Washington, D.C.) 216*, 475–485.
Englund, P. T., Huberman, J. A., Jovin, T. M., & Kornberg, A. (1969a) *J. Biol. Chem. 244*, 3038–3044.
Englund, P. T., Kelly, R. B., & Kornberg, A. (1969b) *J. Biol. Chem. 244*, 3045–3052.
Felsenfeld, G. M., & Miles, H. T. (1967) *Annu. Rev. Biochem. 36*, 407–448.
Ferrin, L. J., & Mildvan, A. S. (1985a) *Biophys. J. 47*, 389a (Abstr.).
Ferrin, L. J., & Mildvan, A. S. (1985b) *Biochemistry 24*, 6904–6913.
Ferrin, L. J., Beckman, R. A., Loeb, L. A., & Mildvan, A. S. (1986) in *Manganese in Metabolism and Enzyme Function* (Schramm, V. L., & Wedler, F. C., Eds.) Academic, New York (in press).
Fry, D. C., Kuby, S. A., & Mildvan, A. S. (1985) *Biochemistry 24*, 4680–4694.
Green, E. A., Rosenstein, R. D., Shiono, R., Abraham, D. J., Trus, B. L., & Marsh, R. E. (1975) *Acta Crystallogr., Sect. B: Struct. Crystallogr. Cryst. Chem. B31*, 102–107.
Haschemeyer, A. E. V., & Sobell, H. M. (1965) *Acta Crystallogr. 19*, 125–130.
Joyce, C. M., & Grindley, N. D. F. (1983) *Proc. Natl. Acad. Sci. U.S.A. 80*, 1830–1834.
Joyce, C. M., Fujii, D. M., Laks, H. S., Hughes, C. M., & Grindley, N. D. F. (1985a) *J. Mol. Biol. 186*, 283–293.
Joyce, C. M., Ollis, D. L., Rush, J., Steitz, T. A., Konigsberg, W. H., & Grindley, N. D. F. (1985b) *U.C.L.A. Symposium on Protein Structure, Function and Design* (in press).
Kalk, A., & Berendsen, H. J. C. (1976) *J. Magn. Reson. 24*, 343–366.
Kan, L. S., Cheng, D. M., Jayaraman, K., Leutzinger, E. E., Miller, P. S., & T'so, P. O. P. (1982) *Biochemistry 21*, 6723–6732.
Karkas, J. D. (1973) *Proc. Natl. Acad. Sci. U.S.A. 70*, 3834–3838.
Karkas, J. D., Stavrianopoulos, J. G., & Chargaff, E. (1972) *Proc. Natl. Acad. Sci. U.S.A. 69*, 398–402.
Keepers, J. W., & James, T. L. (1985) *J. Magn. Reson. 57*, 404–426.
Kelly, W. S., & Grindley, N. D. F. (1976) *Nucleic Acids Res. 3*, 2971–2984.
Kornberg, A. (1980) *DNA Replication*, W. H. Freeman, San Francisco.
Kornberg, A. (1982) *1982 Supplement to DNA Replication*, W. H. Freeman, San Francisco.
Kunkel, T. A., Eckstein, F., Mildvan, A. S., Koplitz, R. M., & Loeb, L. A. (1981) *Proc. Natl. Acad. Sci. U.S.A. 78*, 6734–6738.
Lai, T. F., & Marsh, R. E. (1972) *Acta Crystallogr., Sect. B: Struct. Crystallogr. Cryst. Chem. B28*, 1982–1989.
Leng, M., & Felsenfeld, G. (1966) *J. Mol. Biol. 15*, 455–466.
Levitt, M., & Warshel, A. (1978) *J. Am. Chem. Soc. 100*, 2607–2613.
Loeb, L. A., & Kunkel, T. A. (1982) *Annu. Rev. Biochem. 51*, 429–457.
Ludemann, H. D., Roder, O., Westhof, E., Goldamner, E. V., & Muller, A. (1975) *Biophys. Struct. Mechan. 1*, 121–137.
Maniatis, T., Jeffrey, A., & Van de Sande, H. (1975) *Biochemistry 14*, 3787–3794.
Massefski, W., Jr., & Bolton, P. H. (1985) *J. Magn. Reson. 65*, 526–530.
Mildvan, A. S. (1981) *Philos. Trans. R. Soc. London B293*, 65–74.
Mildvan, A. S., & Loeb, L. A. (1979) *CRC Crit. Rev. Biochem. 6*, 219–244.
Mizrahi, V., Henrie, R. N., Marlier, J. F., Johnson, K. A., & Benkovic, S. J. (1985) *Biochemistry 24*, 4010–4018.
Neidle, S., Kuhlbrandt, W., & Achari, A. (1976) *Acta Crystallogr., Sect. B: Struct. Crystallogr. Cryst. Chem. B32*, 1850–1855.
Ogawa, T., Hirose, S., Okazaki, T., & Okazaki, R. (1977) *J. Mol. Biol. 112*, 121–140.
Ollis, D. L., Brick, P., Hamlin, R., Xuong, N. G., & Steitz, T. A. (1985) *Nature (London) 313*, 762–766.
Pillai, R. P., Tarien, E., Elgavish, G. A., & Eichhorn, G. L. (1985) *Biophys. J. 47*, 178a (Abstr.).
Rich, A., & Raj Bhandary, U. L. (1976) *Annu. Rev. Biochem. 45*, 805–860.
Rosevear, P. R., Bramson, H. N., O'Brian, C., Kaiser, E. T., & Mildvan, A. S. (1983) *Biochemistry 22*, 3439–3447.
Rushizky, G. W., & Mozejko, J. H. (1977) *Anal. Biochem. 77*, 562–566.

Setlow, P. (1974) *Methods Enzymol. 29*, 3–12.
Shieh, H., Berman, H. M., Dabrow, M., & Neidle, S. (1980) *Nucleic Acids Res. 8*, 85–97.
Singer, M. F., Heppel, L. A., Rushizky, G. W., & Sober, H. A. (1962) *Biochim. Biophys. Acta 61*, 474–477.
Slater, J. P., Tamir, I., Loeb, L. A., & Mildvan, A. S. (1972) *J. Biol. Chem. 247*, 6784–6794.
Sloan, D. L., Loeb, L. A., Mildvan, A. S., & Feldmann, R. J. (1975) *J. Biol. Chem. 250*, 8913–8920.
Solomon, I. (1955) *Phys. Rev. 99*, 559–565.
Srikrishnan, T., Fridey, S. M., & Parthasarathy, R. (1979) *J. Am. Chem. Soc. 101*, 3739–3744.
Takusagawa, F., Koetzle, T. F., Srikrishnan, T., & Parthasarathy, R. (1979) *Acta Crystallogr., Sect. B: Struct. Crystallogr. Cryst. Chem. B35*, 1388–1394.
Travaglini, E. C., Mildvan, A. S., & Loeb, L. A. (1975) *J. Biol. Chem. 250*, 8647–8656.
Wagner, G., & Wuthrich, K. (1979) *J. Magn. Reson. 33*, 675–680.
Westergaard, O., Brutlag, D., & Kornberg, A. (1973) *J. Biol. Chem. 248*, 1361–1364.
Young, D. W., Tollin, P., & Wilson, H. R. (1974) *Acta Crystallogr., Sect. B: Struct. Crystallogr. Cryst. Chem. B30*, 2012–2018.

Deuterium Isotope Effects in the Carboxylase Reaction of Ribulose-1,5-bisphosphate Carboxylase/Oxygenase†

Drew E. Van Dyk and John V. Schloss*

Central Research and Development Department, Experimental Station E328, E. I. du Pont de Nemours & Co., Wilmington, Delaware 19898

Received February 3, 1986; Revised Manuscript Received April 21, 1986

ABSTRACT: The deuterium isotope effects on the carboxylase reactions of spinach and *Rhodospirillum rubrum* ribulosebisphosphate carboxylase/oxygenase by [3-^{2}H]ribulose 1,5-bisphosphate have been examined. With the spinach enzyme, the isotope effects observed at high pH on V_{max} and V_{max}/K_m do not vary with CO_2 from moderate concentrations (approximately equal to K_m) to rather high levels (up to 100 times K_m). These results are interpreted in favor of a Theorell–Chance type of kinetic mechanism in which CO_2 adds to the ene–diol of ribulose bisphosphate in a bimolecular fashion after abstraction of the C-3 proton of the sugar bisphosphate. In contrast to the lack of an effect by CO_2, the isotope effect on V_{max} is pH-dependent. The V_{max} isotope effect varies from 2 ($[^1H]V/[^2H]V$) at high pH to about 9 at low pH. The pH dependence of V and V/K for the spinach enzyme is defined by two ionizable groups over the pH range of 6–9. One group, which must be protonated for activity, exhibits a pK of 8.3 ± 0.2 in the V_{max} profile and 7.5 ± 0.4 in the V/K profile. The other group, which must be present as the free base for activity, exhibits a pK of 7.1 ± 0.1 in the V and 7.5 ± 0.4 in the V/K profile. Change in the isotope effect on V correlates with protonation of the latter enzymic group. Inhibition of the spinach enzyme by xylulose 1,5-bisphosphate, a substrate analogue, is also pH-dependent and appears to depend on the correct protonation state of the same or similar enzymic groups as those seen in the V and V/K profiles. Lack of perturbation of either pK by propylene glycol suggests both are cationic acids (lysyl or histidyl residues). In contrast to the spinach enzyme, the isotope effects on both V and V/K are pH-dependent with the corresponding enzyme from *Rhodospirillum rubrum*. The deuterium isotope effect on V varies from 1.5 at high pH to about 5 at low pH, while that on V/K varies from 1 at high pH to about 7 at low pH. Similar pK values were observed for the essential enzymic base with the *R. rubrum* enzyme in both the V and V/K profiles to those observed with the spinach enzyme. These data suggest that the enzymic group with a pK of about 7.5 in both spinach and *R. rubrum* enzymes is the essential enzymic base that abstracts the C-3 proton of ribulose bisphosphate in the first step of the reaction.

Ribulosebisphosphate carboxylase/oxygenase (EC 4.1.1.39) catalyzes the conversion of D-ribulose 1,5-bisphosphate and CO_2 to two molecules of D-3-phosphoglycerate. This reaction is the ultimate means of CO_2 fixation in most photosynthetic organisms [for review, see Akazawa et al. (1978) and Miziorko & Lorimer (1983)]. Molecular oxygen is a competing substrate (vs. CO_2) for this enzyme. Inhibition of the carboxylase reaction by O_2 accounts for the inhibition of photosynthesis by O_2, a physiological response known as the Warburg effect (Bahr & Jensen, 1974; Andrews et al., 1975; Laing et al., 1975; Chollet & Ogren, 1975; Chollet, 1977). As the oxygenase reaction is an energy wasteful process, its elimination would have potential agronomic significance. Plants grown under low oxygen tensions or elevated CO_2 concentrations, to minimize the Warburg effect, have a substantially enhanced growth rate and yield (Hardy et al., 1978). These observations have led to various speculations as to the feasibility of eliminating the oxygenase reaction by either chemical or genetic means (Andrews & Lorimer, 1978; Lorimer & Andrews,

† A preliminary report of these results has been published (Schloss, 1983).

0006-2960/86/0425-5145$01.50/0